

UNIVERSIDAD SAN FRANCISCO DE QUITO
Colegio de Ciencias e Ingeniería

**THE CURVATURE METHOD APPLIED
TO CHARACTERIZE THERMAL
SPRAY COATINGS: ANALYTICAL
LINEAR ELASTIC ANALYSIS**

Bryan Patricio Maldonado Puente

Alfredo Valarezo, Ph.D., Director de Tesis

Tesis de grado presentada como requisito
para la obtención del título de: Ingeniero Mecánico

Quito, mayo 2014

UNIVERSIDAD SAN FRANCISCO DE QUITO

Colegio de Ciencias e Ingeniería

HOJA DE APROBACIÓN DE TESIS

The Curvature Method Applied to Characterize Thermal Spray Coatings: Analytical
Linear Elastic Analysis

Bryan Patricio Maldonado Puente

Alfredo Valarezo, Ph.D.

Director de Tesis

John R. Skukalek, Ph.D.

Miembro del Comité de Tesis

Patricio Chiriboga, Ph.D.

Miembro del Comité de Tesis

Alfredo Valarezo, Ph.D.

Director Departamento de Ingeniería Mecánica

Ximena Córdova, Ph.D.

Decana Escuela de Ingeniería

Colegio de Ciencias e Ingeniería

Quito, mayo 2014

©DERECHOS DE AUTOR

Por medio del presente documento certifico que he leído la Política de Propiedad Intelectual de la Universidad San Francisco de Quito y estoy de acuerdo con su contenido, por lo que los derechos de propiedad intelectual del presente trabajo de investigación quedan sujetos a lo dispuesto en la Política.

Asimismo, autorizo a la USFQ para que realice la digitalización y publicación de este trabajo de investigación en el repositorio virtual, de conformidad a lo dispuesto en el Art. 144 de la Ley Orgánica de Educación Superior.

Firma:

Nombre: Bryan Patricio Maldonado Puente

C.I.: 1720579075

Fecha: Quito, 7 de mayo de 2014

Every problem has in it the seeds of its own solution. If you don't have any problems, you don't get any seeds.

- Norman Vincent Peale

Acknowledgements

I want to thank my thesis advisor Alfredo Valarezo Ph.D in Mechanical Engineering for giving me the support and guidance I needed to continue with my work during this learning process of writing an academic article; since I started with this project I have discovered a new field in mechanic of materials thanks to him. After uncountable hours of work and meetings we have not just finish a pure theoretical article, but most of all, we have enriched our bonds of friendship sharing new experiences and ideas.

To my parents, without whose love and support I would not be able to accomplish my dreams.

Resumen

La proyección térmica es una de las tecnologías de deposición más comunes en la industria de recubrimientos gruesos. Durante la deposición, la deformación térmica entre el sustrato y las capas del recubrimiento desarrolla esfuerzos residuales. El proceso de deposición capa por capa genera esfuerzos de temple y granallado que en el equilibrio a través del espesor de la viga compuesta (recubrimiento/sustrato) genera un perfil de esfuerzos residuales. Bajo supuestos elásticos lineales, un análisis analítico de múltiples capas se presenta en este estudio, con el objetivo de calcular el perfil de esfuerzos después del proceso de deposición y después de enfriar a temperatura ambiente la viga compuesta. El modelo utiliza datos de curvatura-temperatura adquiridos durante el seguimiento *in-situ* del proceso de deposición. El sustrato típico para este proceso es una placa delgada que se dobla por la aparición de esfuerzos residuales. Todos los esfuerzos térmicos producidos durante la deposición debido al calentamiento o enfriamiento del material compuesto se han tomado en cuenta.

Para la caracterización de post-procesamiento, la viga de material compuesto puede ser sometido a un ciclo de calentamiento (ciclos de calentamiento-enfriamiento) para obtener el comportamiento de curvatura-temperatura que depende de las propiedades de expansión de los materiales, y sus respectivos módulos elásticos en el plano. Un análisis analítico para este experimento *ex-situ* se presenta para determinar las propiedades del material de revestimiento, específicamente 1) módulo de elasticidad en el plano y/o 2) el coeficiente de expansión térmica (CTE). Esta información es de alto interés en la mayoría de los casos pues estas propiedades son desconocidas para el material de recubrimiento, o son altamente dependientes del proceso de deposición. Los valores de las propiedades se obtienen como dependientes de la temperatura.

Por último, un análisis de sensibilidad se presenta con el propósito de determinar los parámetros óptimos para llevar a cabo pruebas de curvatura aplicadas a recubrimientos. El espesor del recubrimiento óptimo a espesor del sustrato se sugiere en base a las relaciones de módulos y de CTE. El objetivo es reducir al mínimo los errores relativos en la recopilación de datos curvatura-temperatura durante los experimentos *in-situ* o *ex-situ*.

Abstract

Thermal spray is one of the most common deposition technologies in the industry of thick coatings. During deposition, thermal strain misfit between substrate and coating layers develops residual stresses. The deposition process layer-by-layer generates quenching and peening stress that balance through-thickness of the composite beam (coating/substrate) to produce a profile of residual stresses. Under linear elastic assumptions, an analytic multilayer analysis is presented in this study, aiming to calculate the stress profile after the deposition process and after cooling to room temperature. The model uses curvature-temperature data acquired during the *in-situ* monitoring of the deposition process. The typical sprayed substrate is a thin plate which bends due the occurrence of residual stresses. All thermal stresses produced during deposition due to heating or cooling of the composite are taken into account.

For post-processing characterization, the composite beam can be subjected to a heat cycle (heating-cooling cycles) to obtain the curvature-temperature behavior that is dependent on the expansion properties of the materials, and their respective in-plane elastic moduli. An analytic analysis for this *ex-situ* experiment is presented to determine the properties of the coating material, specifically 1) in-plane elastic modulus and/or 2) the coefficient of thermal expansion (CTE). This is of high interested provided that in most cases, these properties are unknown for the coating material, or are highly dependent on the processing. The property values are obtained as temperature dependent.

Finally, a sensitivity analysis is presented for the purpose of determining the optimum parameters to conduct curvature tests applied to coatings. The optimum coating thickness to substrate thickness is suggested based on the modulus ratios and CTE's. The goal is to minimize relative errors in curvature-temperature data collection during the *in-situ* or *ex-situ* experiments.

Contents

Declaration of Authorship	4
Acknowledgements	6
Resumen	7
Abstract	8
List of Figures	12
List of Tables	14
Symbols	15
1 Introduction	17
2 Residual Stress	20
2.1 Analytic Model for Intrinsic Stresses (quenching + peening) during spraying .	21
2.1.1 Deposition of the first layer	22
2.1.2 Deposition of the second layer	25
2.1.3 Deposition of the n^{th} layer	28
2.1.4 Deposition of m layers on the other side of the substrate	31
2.2 Analytic Model for Thermal Stress (during deposition and post deposition) .	35
2.2.1 Thermal Stresses of n layers on the substrate	35
2.2.2 Thermal Stresses of m layers on the other side of the substrate	37

	10
2.3 Final Stress Distribution	40
2.3.1 Deposition Stage	40
2.3.2 Cooling stage: post spraying	42
2.4 Multilayer model of a coating of a single material	43
2.5 Application: Prediction of intrinsic stresses in bulky parts based on curvature experiment	47
2.5.1 Deposition of the first layer	48
2.5.2 Deposition of the second layer	49
2.5.3 Deposition of the n^{th} layer	50
2.5.4 Deposition of m layers on the other side of the substrate	50
2.5.5 Final stress distribution	51
3 Computer Model	52
3.1 Data Acquisition	54
3.2 Thermal Stress during deposition routine	56
3.3 Evolving Stress routine	57
3.4 Intrinsic Stress routine	57
3.5 Thermal Stress during cooling post-deposition routine	58
3.6 Results	59
3.6.1 Prediction for bulky parts	61
3.6.2 Multilayer system with two different coating materials	62
3.6.3 Multilayer system with one coating material	64
3.7 Architecture	66
4 Calculation of Properties for Coating Materials by the Curvature Method	67
4.1 Determination of mechanical properties for NiCr	70
5 Sensitivity Analysis	72
6 Conclusion	83
Appendix A Proof of Summation Identities	85

	11
Appendix B Program Main Routine	86
Appendix C Data Acquirement	88
Appendix D Cooling Stress Routine	90
Appendix E Heating Stress Routine	92
Appendix F Evolving Stress Routine	94
Appendix G Intrinsic Stress Routine	95
Appendix H Plotting Results Routine	96
Appendix I Subroutines for Thermal Stress Distribution	99
I.1 Young modulus assignation	99
I.2 Neutral axis position	99
I.3 Uniform strain component	100
I.4 Curvature	100
I.5 Stress distribution in substrate	101
I.6 Stress distribution in deposit	102
Appendix J Subroutines for Intrinsic Stress Distribution	104
J.1 Composite beam stiffness	104
J.2 Tensile/Compresive force	105
J.3 Stress distribution in substrate	105
J.4 Stress distribution in deposit	106
Appendix K Subroutines for Quenching Stress Distribution	108
K.1 Quenching stress on deposit	108
K.2 Stoney formula approximation	109
Bibliography	110

List of Figures

2.1	Typical curvature-temperature data in coating processing	21
2.2	Stress assumptions on the process	22
2.3	Forces present in the first layer	23
2.4	Forces present in the second layer	25
2.5	Forces present in the composite beam	31
2.6	Normal strain generated in deposition	48
3.1	Coating process cycles	53
3.2	Schematic description of stress distribution	53
3.3	Data acquired by computer program	56
3.4	Data acquired in deposition	58
3.5	Final stress distribution in thermal spray NiCr on AISI 1018	60
3.6	Comparison between analytic model and Stoney formula (NiCr)	60
3.7	Final stress distribution in thermal spray NiCr on AISI 1018 (bulky)	61
3.8	Data acquired by computer program for two deposition sessions	62
3.9	Final stress distribution in thermal spray YSZ+NiCrAlY on Inconel 718	63
3.10	Comparison between analytic model and Stoney formula (YSZ+NiCrAlY)	63
3.11	Data acquired by computer program for one deposition session	64
3.12	Final stress distribution in thermal spray YSZ on Aluminium	65
3.13	Comparison between analytic model and Stoney formula (YSZ)	65
3.14	Program Diagram	66
4.1	Thermal cycles for NiCr on both, Al6061 and SS316	70
4.2	Elastic modulus and CTE as a function of temperature for NiCr	71

	13
5.1 3D plot for the function $f(x, y)$	74
5.2 Contour plot for the function $f(x, y)$	75
5.3 3D plot for the function $M_x(x, y)$	76
5.4 3D plot for the function $M_y(x, y)$	77
5.5 Negligible region for $M_x(x, y)$ and $M_y(x, y)$	77
5.6 Values for $M_x(x, y)$ and $M_y(x, y)$ in first region	78
5.7 Values for $M_x(x, y)$ and $M_y(x, y)$ in second region	79
5.8 Values for $f(x, y)$ in third region	79
5.9 Values for $M_x(x, y)$ in third region	80
5.10 Values for $M_y(x, y)$ in third region	80
5.11 Values for $M_x(x, y)$ and $M_y(x, y)$ in third region	81

List of Tables

3.1	Input data comparison between Tsui-Clyne model and multilayer analytic model	55
3.2	Parameters used in deposition of NiCr on AISI1018	59
3.3	Parameters used in deposition of YSZ+NiCrAlY on Inconel 718	62
3.4	Parameters used in deposition of YSZ on Aluminium	64
4.1	Parameters used for thermal cycle calculations	70
5.1	Actions to take given the value of $y = E_s/E_d$	81

Symbols

$\sigma_{x/y/z}$	Stress in direction $x/y/z$	Pa
$\varepsilon_{x/y/z}$	Elastic strain in direction $x/y/z$	–
$\varepsilon_{s/d}$	Elastic strain of substrate/deposit	–
$E_{s/d}$	Elastic modulus of substrate/deposit	Pa
$\nu_{s/d}$	Poisson ratio of substrate/deposit	–
t_s	Substrate thickness	m
t_i	Thickness of layer i	m
F_i	Normal force due to deposition of layer i	N
M_i	Bending moment due to deposition of layer i	N m
y	Displacement through the thickness of the beam	m
δ_i	Neutral axis position for composite beam with i layers	m
$\Delta\kappa_i$	Curvature change due to deposition of layer i	m^{-1}
E_y	Effective elastic modulus at position y	Pa
S_i	Flexural stiffness for composite beam with i layers	Pa m^4
b	Substrate width	m
$\sigma_{(s,i)}$	Stress distribution in substrate after i^{th} layer	Pa
$\sigma_{(j,i)}$	Stress distribution in layer j after i^{th} layer	Pa
$t_{(s,i)}$	Substrate equivalent thickness for i^{th} deposition	m
$t_{(j,i)}$	Equivalent thickness for layer j at the i^{th} deposition	m
n	Number of layers	–
h_n	Coating thickness after deposition on n layers	m
$\Delta\kappa_T$	Curvature change due to temperature gradient	m^{-1}
ε_n	Elastic strain at cooling/heating composite beam	–
c_n	Uniform strain component due to cooling/heating force	–
ΔT_n	Temperature gradient at cooling/heating	$^{\circ}\text{C}$
α_s	Coefficient of thermal expansion for substrate	K^{-1}
α_i	Coefficient of thermal expansion for layer i	K^{-1}

$\sigma_s(1)$	Stress at the top of the substrate after deposition	Pa
$\sigma_s(2)$	Stress at the bottom of the substrate after deposition	Pa
$\sigma_d(i)$	Stress at the midpoint of layer i after deposition	Pa
$\sigma_{(s,c)}(1)$	Stress at the top of the substrate after cooling	Pa
$\sigma_{(s,c)}(2)$	Stress at the bottom of the substrate after cooling	Pa
$\sigma_{(d,c)}(i)$	Stress at the midpoint of layer i after cooling	Pa
$\sigma_{(q,i)}$	Quenching stress due to deposition of layer i	Pa
σ_{ev}	Stoney formula stress	Pa
$\Delta\varepsilon$	Misfit strain	–
$\sim \mathcal{O}(n)$	Order of magnitude similar to n	

Chapter 1

Introduction

Thermal spray (TS) is a well-known technology to deposit coatings. This technique is used to deposit coatings that resist wear, friction, heat, corrosion, etc [1–3]. As in every manufacturing process, there exists intrinsic residual stresses that may affect the performance of a coated component. Basically, a typical TS technique incorporates a torch that heats up a feedstock material, fed into the torch in the form of particles or wire. The material is melted by the torch and projected to the substrate.

The origin of residual stress in TS is based on thermal contraction, impact, and differential expansion of the substrate material and the deposit [4–9]. The material is formed as projected molten droplets are laid down over the substrate in the shape of splats. The splats solidify and cool down causing a large change in volume that originates residual stresses, tensile in nature. When particles are projected at high velocities, they impact on substrates creating plastic deformation and determining compressive residual stresses. When the coating deposition ends, the coated component has gained heat and ends up hot (i.e to 250-400 °C). The coated component cools down to room temperature, creating a differential contraction as the coefficient of thermal expansion (CTE) often differs between substrate and coating. This is another source of residual stresses that can be either tensile or compressive depending upon

the CTE values. The differential thermal contraction may also occur during processing due to the periodic rastering of the torch over the part causing heating and cooling cycles.

It is of high interest to measure and reduce residual stresses in the coatings. A common procedure to measure stresses is to deposit the coatings over thin plates, representative of the material of the component. Due to the presence of residual stresses, the plate bends uniformly in such a way that a single radius of curvature characterizes the amount of residual stress stored in the system. Instrumented sensors have been developed and used for monitoring the curvature of thin plates *in-situ* during spraying [10]. A commercial sensor is available and commercialized by Reliacoat L.L.C (NY, USA). The sensor provides curvature measurements and temperature in real-time during deposition of coatings. The curvature information is processed to predict the resultant residual stress condition of the coating, and substrate. The principle of measurement of residual stresses via the curvature method has been described and used in several papers [10,11]. However, there is no publication that describes thoroughly an analytical linear elastic model to obtain the residual stress in a coating/substrate sample based on the input of curvature-temperature data. The present study is compelling as it considers the deposit of multilayered coatings (e.g. layers of different materials), on both sides of the substrate, thermal changes during processing and cooling, etc.

Concurrently, an analytical linear elastic model to obtain coating properties, specifically CTE, and elastic modulus, is also described. The monitoring of curvature and temperature can be used during *ex-situ* thermal cycles to obtain these properties [5,10]. The procedure is used to obtain the properties that are required for the *in-situ* model of residual stresses.

Tsui-Clyne [12] developed an analytical model to predict the residual stress distribution in progressively deposited coatings. The model considers as input the amount of intrinsic (quenching) stress developed. This is often a difficult magnitude to be estimated a-priori and thus, it is necessary to measure it. In another contribution, Hsueh [13] developed the theoretical analysis to solve the stress distribution in a multi-material layered composite beam

subjected to heating/cooling cycles. In the present study, the analytic linear elastic analysis for a multi-material layered coating is developed using the theoretical solutions of mechanics of solids from both [13] and [12]. The solution considers intrinsic and thermal stress; and the solution of CTE and elastic modulus of a composite plate. A detailed analysis is also presented to investigate the sensitivity of the procedure to measurement errors that may arise during the experimental determination of curvature, temperature, thicknesses, etc. The analysis also suggests optimum combinations of thickness ratios, modulus ratios, etc, between coating and substrate to enhance the reliability of the measurements.

In Chapter 2 the analytic model for the *in-situ* experiment is developed. Every layer being deposited will induce an amount of stress in the composite beam. The intrinsic stress for a multilayer deposition system is developed in Section 2.1. At the end of the section, a general solution for a substrate sprayed from both sides is presented. The final residual stress distribution through the thickness is presented by adding the thermal stress during *in-situ* deposition and during cooling, to the intrinsic stress.

The complexity of the residual stress distribution solutions demands the development of a computer program to reach the solution automatically. Chapter 3 explains the architecture of the computer model implemented in MATLAB[®]. Results for several coatings/substrate systems are presented, for instance NiCr coating deposited over AISI 1018 steel, YSZ onto aluminium substrate, etc. The architecture of the program is presented in Figure 3.14 and every routine and subroutine needed in order to calculate the residual stress and the intrinsic stresses are presented in Appendices B to K.

Chapter 4 presents theoretical solutions to extract the mechanical properties, specifically the elastic modulus of coatings. Also, a novel application of the curvature method to obtain the CTE of the coating is presented by analyzing the *ex-situ* experimental data of temperature and curvature of the desired coating deposited onto two different substrates. An example of the deposition of NiCr over Al6061 and over SS316 is presented.

Chapter 2

Residual Stress

Residual stresses are commonly generated during coating processing. As the coating is deposited over one side of a thin plate, the coating/substrate system adopts a curvature to balance the moment produced by the intrinsic stresses: quenching and peening stress. [14] Often during coating deposition thermal gradients occur due to cooling of the part. This is a source of thermal stresses that usually are not taken into account in previous analysis [12] but are considered here. Lately, during the coating processing there will be a residual stress distribution through the thickness due to deposition stress (intrinsic + thermal) and cooling stress (only thermal). An analytic model for residual stress distribution for a multilayer progressively deposited coating systems is presented.

It is assumed that both substrate and coatings behave as linear elastic solids. In addition to the analytic model presented in [13] and [12], here the analytical solution is applicable to:

1. a multilayer system subjected to stress of different materials
2. a system subjected to spraying where intrinsic and thermal stresses produce a profile
3. the curvature caused by the stresses is feed into the model as a known variable

A typical curvature-temperature data as a function of time for a coating processing is presented in Figure 2.1.

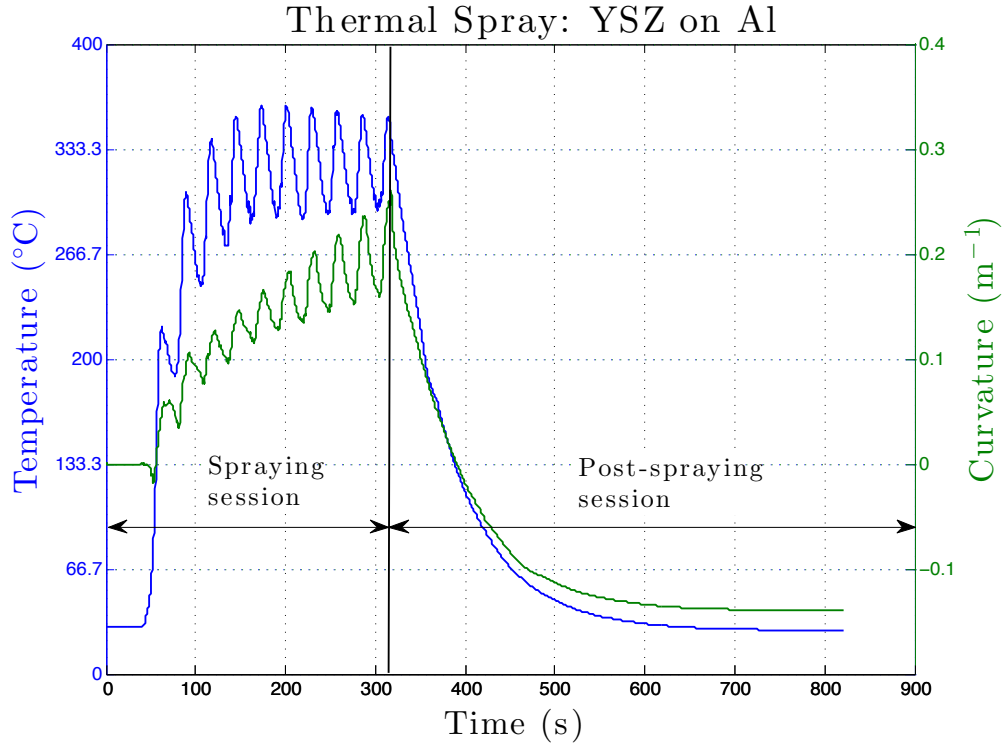


FIGURE 2.1: Curvature-temperature data in coating processing

2.1 Analytic Model for Intrinsic Stresses (quenching + peening) during spraying

The stress developed during the coating processing is due to the misfit strain caused by quenching and peening stress. An equally biaxial stress state ($\sigma_x = \sigma_z$), with negligible through thickness stress ($\sigma_y = 0$), is assumed. The analysis will be developed for a strip shaped substrate where the length is assume to be 10 times longer than the width ($L/b \approx 10$ as in Figure 2.2). Therefore, the analysis will be concentrated in determining the stress through the thickness with a major dimension in the x -direction. The intrinsic stress will

induce a strain in the x -direction (Figure 2.2), due to a Poisson effect. [12] The net strain in the x -direction can thus be written as:

$$\varepsilon_x E = \sigma_x - \nu(\sigma_y + \sigma_z) = \sigma_x(1 - \nu)$$

therefore,

$$\frac{\sigma_x}{\varepsilon_x} = \frac{E}{1 - \nu} = E_{eff}$$

This effective Young's modulus value is going to be used in the following equations.

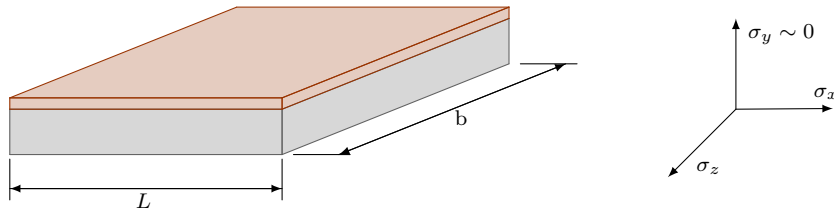


FIGURE 2.2: Stress conditions during deposition

2.1.1 Deposition of the first layer

Once the first layer is deposited on the substrate, a tensile force acts on the deposit while a compressive force of the same magnitude acts on the substrate¹. This pair of equal and opposite forces generates a bending moment. Both forces act on the neutral axis of both substrate and deposit. Figure 2.3 shows a representation of the applied forces. Note that the neutral axis for both substrate and deposit are their middle sections. The interface between the substrate and the deposit is the origin for the y axis.

Note that the lever arm for the bending moment is $t_s/2 + t_1/2$ with respect to $y = 0$, then

$$M_1 = F_1 \left(\frac{t_s}{2} + \frac{t_1}{2} \right) \quad (2.1)$$

¹The force can be tensile or compressive depending upon the dominance of quenching or peening. For a general solution the equations are derived as tensile.

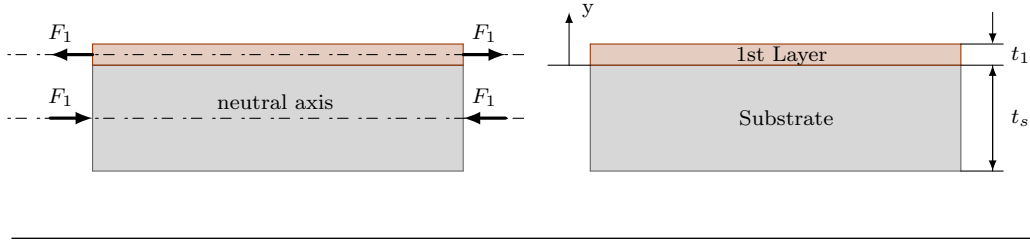


FIGURE 2.3: Force acting product of the deposition of the first layer

On the other hand, the resultant force due to the bending strain component must be zero, then: [13]

$$\begin{aligned} \int_{-t_s}^{t_1} \sigma b \, dy &= 0 \\ b \int_{-t_s}^{t_1} E_y \varepsilon \, dy &= 0 \\ b \int_{-t_s}^{t_1} E_y (y - \delta_1) \Delta \kappa_1 \, dy &= 0 \end{aligned}$$

Where E_y is the effective Young's modulus as a function of the position, δ_1 is the neutral axis of the composite beam, b is the substrate width, and $\Delta \kappa_1$ is the change of curvature generated by the pure bending moment after deposition of the first layer.

$$\begin{aligned} \int_{-t_s}^0 E_s (y - \delta_1) \Delta \kappa_1 \, dy + \int_0^{t_1} E_1 (y - \delta_1) \Delta \kappa_1 \, dy &= 0 \\ E_s \left[\frac{y^2}{2} - \delta_1 y \right]_{-t_s}^0 + E_1 \left[\frac{y^2}{2} - \delta_1 y \right]_0^{t_1} &= 0 \\ -E_s \left(\frac{t_s^2}{2} + \delta_1 t_s \right) + E_1 \left(\frac{t_1^2}{2} - \delta_1 t_1 \right) &= 0 \\ \frac{-E_s t_s^2 + E_1 t_1^2}{2} - \delta_1 (E_s t_s + E_1 t_1) &= 0 \end{aligned}$$

Finally, the neutral axis position for the composite beam is:

$$\delta_1 = \frac{-E_s t_s^2 + E_1 t_1^2}{2(E_s t_s + E_1 t_1)}$$

The composite beam stiffness can be calculated as follows:

$$\begin{aligned}
S_1 &= b \int_{-t_s}^{t_1} E_y (y - \delta_1)^2 dy \\
&= b \left(\int_{-t_s}^0 E_s (y - \delta_1)^2 dy + \int_0^{t_1} E_1 (y - \delta_1)^2 dy \right) \\
&= b \left(E_s \frac{(-\delta_1)^3 - (-t_s - \delta_1)^3}{3} + E_1 \frac{(t_1 - \delta_1)^3 - (-\delta_1)^3}{3} \right) \\
&= b \left(E_s \frac{-\delta_1^3 + t_s^3 + 3t_s^2\delta_1 + 3t_s\delta_1^2 + \delta_1^3}{3} + E_1 \frac{t_1^3 - 3t_1^2\delta_1 + 3t_1\delta_1^2 - \delta_1^3 + \delta_1^3}{3} \right) \\
\frac{S_1}{b} &= E_s t_s \left(\frac{t_s^2}{3} + t_s \delta_1 + \delta_1^2 \right) + E_1 t_1 \left(\frac{t_1^2}{3} - t_1 \delta_1 + \delta_1^2 \right)
\end{aligned}$$

Thus, the change of curvature can be calculated as:

$$\Delta\kappa_1 = \frac{M_1}{S_1} \quad (2.2)$$

Since curvature is used as an input, the force generated by the misfit strain can be calculated using Equations 2.1 and 2.2 as follows:

$$\begin{aligned}
\frac{F_1}{b} &= \frac{M_1}{b} \left(\frac{t_s + t_1}{2} \right)^{-1} \\
&= \frac{S_1}{b} \Delta\kappa_1 \left(\frac{t_s + t_1}{2} \right)^{-1}
\end{aligned}$$

Let $\sigma_{(s,1)}(y)$ be the stress distribution in the substrate as a result of the deposition of the first layer. This stress is composed of the portion due to the curvature with respect to the neutral axis ($-E_s \Delta\kappa_1 (y - \delta_1)$) and the portion due to the intrinsic stresses ($-\frac{F_1}{bt_s}$). Thus, for $y \in [-t_s, 0]$ the distribution can be calculated as:

$$\sigma_{(s,1)}(y) = -\frac{F_1}{bt_s} - E_s \Delta\kappa_1 (y - \delta_1)$$

Similarly, let $\sigma_{(1,1)}(y)$ be the stress distribution in the first layer. For $y \in [0, t_1]$ the distribution is:

$$\sigma_{(1,1)}(y) = \frac{F_1}{bt_1} - E_1 \Delta \kappa_1 (y - \delta_1)$$

2.1.2 Deposition of the second layer

Once the first layer has solidified on the substrate, the second layer will generate again a residual stress due to misfit strain. A tensile force F_2 acting on the new coating layer and the substrate + first layer beam of equal and opposite magnitude generates a bending moment. Note that F_2 is not necessarily equal to F_1 , this will depend on the actual curvature measured. This force will act on the neutral axis of the composite beam (δ_1) and the middle section of the new layer. Figure 2.4 shows a representation of the applied forces.

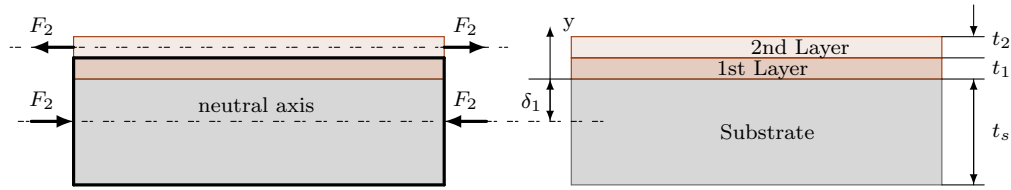


FIGURE 2.4: Force acting product of the deposition of the second layer

Note that the lever arm for the bending moment is $(t_1 - \delta_1) + t_2/2$ with respect to $y = 0$, then

$$M_2 = F_2(t_1 - \delta_1 + t_2/2) \quad (2.3)$$

The resultant force due to the bending strain component must be zero, then: [13]

$$\int_{-t_s}^{t_1+t_2} E_y(y - \delta_2) \Delta \kappa_2 dy = 0$$

Where E_y is the effective Young's modulus as a function of the position, δ_2 is the neutral axis of the new composite beam and $\Delta\kappa_2$ is the curvature generated by deposition of the second layer.

$$\begin{aligned}
\int_{-t_s}^0 E_s(y - \delta_2)\Delta\kappa_2 dy + \int_0^{t_1} E_1(y - \delta_2)\Delta\kappa_2 dy + \int_{t_1}^{t_1+t_2} E_2(y - \delta_2)\Delta\kappa_2 dy &= 0 \\
E_s \left[\frac{y^2}{2} - \delta_2 y \right]_{-t_s}^0 + E_1 \left[\frac{y^2}{2} - \delta_2 y \right]_0^{t_1} + E_2 \left[\frac{y^2}{2} - \delta_2 y \right]_{t_1}^{t_1+t_2} &= 0 \\
-E_s \left(\frac{t_s^2}{2} + \delta_2 t_s \right) + E_1 \left(\frac{t_1^2}{2} - \delta_2 t_1 \right) + E_2 \left(\frac{(t_1 + t_2)^2}{2} - \delta_2(t_1 + t_2) - \frac{t_1^2}{2} + \delta_2 t_1 \right) &= 0 \\
-E_s \left(\frac{t_s^2}{2} + \delta_2 t_s \right) + E_1 \left(\frac{t_1^2}{2} - \delta_2 t_1 \right) + E_2 \left(t_1 t_2 + \frac{t_2^2}{2} - \delta_2 t_2 \right) &= 0 \\
\frac{-E_s t_s^2 + E_1 t_1^2 + E_2 t_2(2t_1 + t_2)}{2} - \delta_2(E_s t_s + E_1 t_1 + E_2 t_2) &= 0
\end{aligned}$$

Finally, the neutral axis position for the composite beam is:

$$\delta_2 = \frac{-E_s t_s^2 + E_1 t_1^2 + E_2 t_2(2t_1 + t_2)}{2(E_s t_s + E_1 t_1 + E_2 t_2)}$$

The composite beam stiffness can be calculated as follows:

$$\begin{aligned}
S_2 &= b \int_{-t_s}^{t_1+t_2} E_y(y - \delta_2)^2 dy \\
&= b \left(\int_{-t_s}^0 E_s(y - \delta_2)^2 dy + \int_0^{t_1} E_1(y - \delta_2)^2 dy + \int_{t_1}^{t_1+t_2} E_2(y - \delta_2)^2 dy \right) \\
&= b \left(E_s \frac{(-\delta_2)^3 - (-t_s - \delta_2)^3}{3} + E_1 \frac{(t_1 - \delta_2)^3 - (-\delta_2)^3}{3} + E_2 \frac{(t_1 + t_2 - \delta_2)^3 - (t_1 - \delta_2)^3}{3} \right) \\
&= b \left(E_s \frac{-\delta_2^3 + t_s^3 + 3t_s^2\delta_2 + 3t_s\delta_2^2 + \delta_2^3}{3} + E_1 \frac{t_1^3 - 3t_1^2\delta_2 + 3t_1\delta_2^2 - \delta_2^3 + \delta_2^3}{3} \right. \\
&\quad \left. + E_2 t_2 \frac{(t_1 + t_2 - \delta_2)^2 + (t_1 + t_2 - \delta_2)(t_1 - \delta_2) + (t_1 - \delta_2)^2}{3} \right) \\
\frac{S_2}{b} &= E_s t_s \left(\frac{t_s^2}{3} + t_s \delta_2 + \delta_2^2 \right) + E_1 t_1 \left(\frac{t_1^2}{3} - t_1 \delta_2 + \delta_2^2 \right) \\
&\quad + E_2 t_2 \frac{(t_1 + t_2)^2 - 2(t_1 + t_2)\delta_2 + \delta_2^2 + (t_1 + t_2)t_1 - (t_1 + t_2)\delta_2 - t_1\delta_2 + \delta_2^2 + t_1^2 - 2t_1\delta_2 + \delta_2^2}{3}
\end{aligned}$$

$$\begin{aligned} \frac{S_2}{b} &= E_s t_s \left(\frac{t_s^2}{3} + t_s \delta_2 + \delta_2^2 \right) + E_1 t_1 \left(\frac{t_1^2}{3} - t_1 \delta_2 + \delta_2^2 \right) \\ &\quad + E_2 t_2 \left(\frac{(t_1 + t_2)^2 + (t_1 + t_2)t_1 + t_1^2}{3} - ((t_1 + t_2) + t_1)\delta_2 + \delta_2^2 \right) \end{aligned}$$

Thus, the change of curvature can be computed as:

$$\Delta\kappa_2 = \frac{M_2}{S_2} \quad (2.4)$$

Since curvature is used as an input, the force generated by the misfit strain can be calculated using Equations 2.3 and 2.4 as follows:

$$\begin{aligned} \frac{F_2}{b} &= \frac{M_2}{b} (t_1 - \delta_1 + t_2/2)^{-1} \\ &= \frac{S_2}{b} \Delta\kappa_2 (t_1 - \delta_1 + t_2/2)^{-1} \end{aligned}$$

In order to calculate the stress distribution as a result of the misfit strain caused by the deposition of the second layer, it is necessary to compute the equivalent substrate and deposit thickness in the composite beam as follows:

$$t_{(s,2)} = \frac{E_s t_s + E_1 t_1}{E_s} \quad \text{and} \quad t_{(1,2)} = \frac{E_s t_s + E_1 t_1}{E_1}$$

Same as before, let $\sigma_{(s,2)}(y)$ be the stress distribution in the substrate after deposition of the second layer. For $y \in [-t_s, 0]$:

$$\sigma_{(s,2)}(y) = \underbrace{-\frac{F_1}{bt_s} - E_s \Delta\kappa_1 (y - \delta_1)}_{\text{due to first layer}} - \underbrace{\frac{F_2}{bt_{(s,2)}} - E_s \Delta\kappa_2 (y - \delta_2)}_{\text{due to second layer}}$$

Similarly, let $\sigma_{(1,2)}(y)$ the stress distribution in the first layer after the deposition of the second layer. For $y \in [0, t_1]$:

$$\sigma_{(1,2)}(y) = \underbrace{\frac{F_1}{bt_1} - E_1 \Delta \kappa_1 (y - \delta_1)}_{\text{due to first layer}} - \underbrace{\frac{F_2}{bt_{(1,2)}} - E_1 \Delta \kappa_2 (y - \delta_2)}_{\text{due to second layer}}$$

Finally, for $y \in [t_1, t_1 + t_2]$ the stress in the second layer can be written as:

$$\sigma_{(2,2)}(y) = \frac{F_2}{bt_2} - E_2 \Delta \kappa_2 (y - \delta_2)$$

2.1.3 Deposition of the n^{th} layer

Lets define the following variable:

$$h_n = \sum_{j=0}^n t_j$$

where $t_0 = 0$. Then, bending moment is:

$$M_n = F_n (h_{n-1} - \delta_{n-1} + t_n/2) \quad (2.5)$$

Recall that $\delta_0 = t_s/2$. The resultant force due to the bending strain component must be zero, then:

$$\begin{aligned} \int_{-t_s}^{h_n} E_y (y - \delta_n) \Delta \kappa_n dy &= 0 \\ \int_{-t_s}^0 E_s (y - \delta_n) \Delta \kappa_n dy + \sum_{j=1}^n \int_{h_{j-1}}^{h_j} E_j (y - \delta_n) \Delta \kappa_n dy &= 0 \\ E_s \left[\frac{y^2}{2} - \delta_n y \right]_{-t_s}^0 + \sum_{j=1}^n E_j \left[\frac{y^2}{2} - \delta_n y \right]_{h_{j-1}}^{h_j} &= 0 \\ -E_s \left(\frac{t_s^2}{2} + \delta_n t_s \right) + \sum_{j=1}^n E_j \left(\frac{h_j^2}{2} - \delta_n h_j - \frac{h_{j-1}^2}{2} + \delta_n h_{j-1} \right) &= 0 \end{aligned}$$

$$\begin{aligned}
-E_s \left(\frac{t_s^2}{2} + \delta_n t_s \right) + \sum_{j=1}^n E_j \left(\frac{(h_j + h_{j-1})(h_j - h_{j-1})}{2} - \delta_n t_j \right) &= 0 \\
-E_s \left(\frac{t_s^2}{2} + \delta_n t_s \right) + \sum_{j=1}^n E_j t_j \left(\frac{(2h_{j-1} + t_j)}{2} - \delta_n \right) &= 0 \\
-E_s t_s^2 + \sum_{j=1}^n E_j t_j (2h_{j-1} + t_j) - 2\delta_n \left(E_s t_s + \sum_{j=1}^n E_j t_j \right) &= 0
\end{aligned}$$

Finally, the neutral axis position for the composite beam is:

$$\delta_n = \frac{-E_s t_s^2 + \sum_{j=1}^n E_j t_j (2h_{j-1} + t_j)}{2 \left(E_s t_s + \sum_{j=1}^n E_j t_j \right)}$$

The composite beam stiffness can be calculated as follows:

$$\begin{aligned}
S_n &= b \int_{-t_s}^{h_n} E_y (y - \delta_n)^2 dy \\
&= b \left(\int_{-t_s}^0 E_s (y - \delta_n)^2 dy + \sum_{j=1}^n \int_{h_{j-1}}^{h_j} E_j (y - \delta_n)^2 dy \right) \\
&= b \left(E_s \frac{(-\delta_n)^3 - (-t_s - \delta_n)^3}{3} + \sum_{j=1}^n E_j \frac{(h_j - \delta_n)^3 - (h_{j-1} - \delta_n)^3}{3} \right) \\
&= b \left(E_s \frac{-\delta_n^3 + t_s^3 + 3t_s^2 \delta_n + 3t_s \delta_n^2 + \delta_n^3}{3} \right. \\
&\quad \left. + \sum_{j=1}^n E_j t_j \frac{(h_j - \delta_n)^2 + (h_j - \delta_n)(h_{j-1} - \delta_n) + (h_{j-1} - \delta_n)^2}{3} \right) \\
\frac{S_n}{b} &= E_s t_s \left(\frac{t_s^2}{3} + t_s \delta_n + \delta_n^2 \right) \\
&\quad + \sum_{j=1}^n E_j t_j \frac{h_j^2 - 2h_j \delta_n + \delta_n^2 + h_j h_{j-1} - h_j \delta_n - h_{j-1} \delta_n + \delta_n^2 + h_{j-1}^2 - 2h_{j-1} \delta_n + \delta_n^2}{3} \\
\frac{S_n}{b} &= E_s t_s \left(\frac{t_s^2}{3} + t_s \delta_n + \delta_n^2 \right) + \sum_{j=1}^n E_j t_j \left(\frac{h_j^2 + h_j h_{j-1} + h_{j-1}^2}{3} - (h_j + h_{j-1}) \delta_n + \delta_n^2 \right)
\end{aligned}$$

Thus, the change of curvature can be calculated as:

$$\Delta\kappa_n = \frac{M_n}{S_n} \quad (2.6)$$

The normal force generated by the misfit strain can be calculated using Equations 2.5 and 2.6, and using the curvature as a known input as follows:

$$\begin{aligned} \frac{F_n}{b} &= \frac{M_n}{b} (h_{n-1} - \delta_{n-1} + t_n/2)^{-1} \\ &= \frac{S_n}{b} \Delta\kappa_n (h_{n-1} - \delta_{n-1} + t_n/2)^{-1} \end{aligned}$$

In order to calculate the stress distribution as a result of the misfit strain caused by the deposition of the n^{th} layer, it is necessary to compute the equivalent substrate and deposit thickness in the composite beam as follows:

$$t_{(s,n)} = \frac{E_s t_s + \sum_{j=1}^{n-1} E_j t_j}{E_s} \quad \text{and} \quad t_{(i,n)} = \frac{E_s t_s + \sum_{j=1}^{n-1} E_j t_j}{E_i}$$

where $t_{(s,n)}$ is the equivalent substrate thickness for the composite beam after deposition of $n - 1$ layers, note that $t_{(s,1)} = t_s$. Similarly, $t_{(i,n)}$ is the equivalent deposit thickness for the i^{th} layer in the composite beam after deposition of $n - 1$ layers. Note that $t_{(n,n)} = t_n$. Then, the stress distribution in the substrate after deposition of n layers is:

$$\sigma_{(s,n)}(y) = - \sum_{j=1}^n \frac{F_j}{b} (t_{(s,j)})^{-1} + E_s \Delta\kappa_j (y - \delta_j)$$

for $y \in [-t_s, 0]$. Similarly, for $y \in [h_{i-1}, h_i]$ the stress distribution in the i^{th} layer after deposition of n layers can be calculated as:

$$\sigma_{(i,n)}(y) = \frac{F_i}{b} t_i^{-1} - E_i \Delta\kappa_i (y - \delta_i) - \sum_{j=i+1}^n \frac{F_j}{b} (t_{(i,j)})^{-1} + E_i \Delta\kappa_j (y - \delta_j)$$

2.1.4 Deposition of m layers on the other side of the substrate

The analytical analysis for the deposition of n layers on one side of the substrate has already been shown. The solution to deposit m layers of different materials on the other side of the substrate is developed as follows. The sequence of calculation will be the same as before. The stress distribution when the m^{th} layer is deposited on the other side of the substrate will be presented. Figure 2.5 illustrates how the deposition of the m^{th} layer in the opposite side generates a tensile/compressive force and a bending moment.

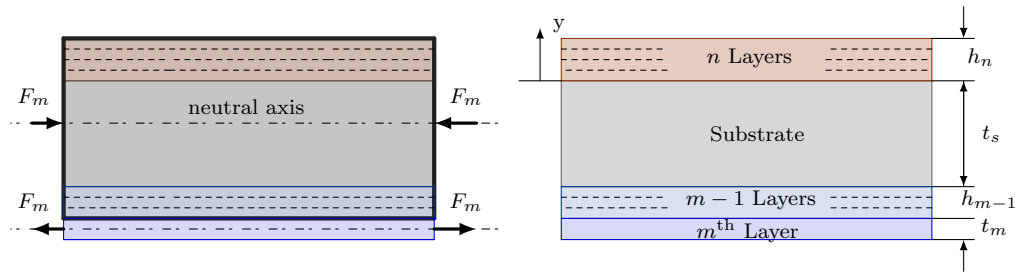


FIGURE 2.5: Force acting product of the deposition of the m^{th} layer on the opposite side

Same as before, the following variable is defined:

$$h_m = \sum_{j=0}^m t_j$$

where t_j is the thickness of the j^{th} layer in the opposite side. Then, the lever arm for the bending moment is:

$$M_m = F_m(h_{m-1} + \delta_{m-1} + t_s + t_m/2)$$

In this case $\delta_0 = \delta_n$, where δ_n is the neutral axis after the deposition of the n^{th} layer in one side, as described in Section 2.1.3. The resultant force due to the bending strain component must be zero, then:

$$\int_{-h_m-t_s}^{h_n} E_y(y - \delta_m)\Delta\kappa_m dy = 0$$

$$\begin{aligned}
\Delta\kappa_m \left[\sum_{j=1}^m \int_{-h_j-t_s}^{-h_{j-1}-t_s} E_j(y-\delta_m)dy + \int_{-t_s}^{h_n} E_y(y-\delta_m)dy \right] &= 0 \\
\sum_{j=1}^m E_j \left[\frac{y^2}{2} - \delta_m y \right]_{-h_j-t_s}^{-h_{j-1}-t_s} + \int_{-t_s}^{h_n} E_y(y-\delta_m)dy &= 0 \\
\sum_{j=1}^m E_j \left(\frac{(h_j+h_{j-1}+2t_s)(-t_j)}{2} - \delta_m t_j \right) + \int_{-t_s}^{h_n} E_y(y-\delta_m)dy &= 0 \\
-\sum_{j=1}^m E_j t_j \left(\frac{(2h_{j-1}+t_j)}{2} \right) - t_s \sum_{j=1}^m E_j t_j - \delta_m \sum_{j=1}^m E_j t_j + \int_{-t_s}^{h_n} E_y(y-\delta_m)dy &= 0 \\
-\sum_{j=1}^m E_j t_j (2h_{j-1}+t_j) - 2t_s \sum_{j=1}^m E_j t_j - 2\delta_m \sum_{j=1}^m E_j t_j & \\
+ \sum_{j=1}^n E_j t_j (2h_{j-1}+t_j) - E_s t_s^2 - 2\delta_m (E_s t_s + \sum_{j=1}^n E_j t_j) &= 0
\end{aligned}$$

Therefore,

$$\delta_m = \frac{\sum_{j=1}^n E_j t_j (2h_{j-1}+t_j) - \sum_{j=1}^m E_j t_j (2h_{j-1}+t_j) - t_s \left(E_s t_s + 2 \sum_{j=1}^m E_j t_j \right)}{2 \left(E_s t_s + \sum_{j=1}^n E_j t_j + \sum_{j=1}^m E_j t_j \right)}$$

Remark 2.1. Note that if n layers are deposited on one side of the substrate and then, the same n layers are deposited on the other side of the substrate then, $\delta_m = -t_s/2$, which means there would not be any bending moment acting on the composite beam during heat cycle. The neutral axis would agree with the geometrical centroid.

The composite beam stiffness with respect to the neutral axis δ_m can be calculated as:

$$\begin{aligned}
S_m &= b \int_{-h_m-t_s}^{h_n} E_y(y-\delta_m)^2 dy \\
\frac{S_m}{b} &= \sum_{j=1}^m \int_{-h_j-t_s}^{-h_{j-1}-t_s} E_j(y-\delta_m)^2 dy + \int_{-t_s}^{h_n} E_y(y-\delta_m)^2 dy \\
\frac{S_m}{b} &= \sum_{j=1}^m E_j \frac{(-h_{j-1}-t_s-\delta_m)^3 - (-h_j-t_s-\delta_m)^3}{3} + \int_{-t_s}^{h_n} E_y(y-\delta_m)^2 dy
\end{aligned}$$

$$\begin{aligned}
\frac{S_m}{b} &= \sum_{j=1}^m E_j t_j \frac{(h_{j-1} + t_s + \delta_m)^2 + (h_{j-1} + t_s + \delta_m)(h_j + t_s + \delta_m) + (h_j + t_s + \delta_m)^2}{3} \\
&\quad + \int_{-t_s}^{h_n} E_y (y - \delta_m)^2 dy \\
\frac{S_m}{b} &= \sum_{j=1}^m E_j t_j \frac{(h_{j-1} + t_s + \delta_m)^2 + (h_{j-1} + t_s + \delta_m)(h_j + t_s + \delta_m) + (h_j + t_s + \delta_m)^2}{3} \\
&\quad + \int_{-t_s}^{h_n} E_y (y - \delta_m)^2 dy \\
\frac{S_m}{b} &= \sum_{j=1}^m E_j t_j \left(\frac{h_j^2 + h_j h_{j-1} + h_{j-1}^2}{3} + (h_j + h_{j-1})\delta_m + \delta_m^2 + t_s^2 + t_s(h_j + h_{j-1}) + 2t_s\delta_m \right) \\
&\quad + \int_{-t_s}^{h_n} E_y (y - \delta_m)^2 dy
\end{aligned}$$

Thus,

$$\begin{aligned}
\frac{S_m}{b} &= E_s t_s \left(\frac{t_s^2}{3} + t_s \delta_m + \delta_m^2 \right) + \sum_{j=1}^m E_j t_j (t_s^2 + t_s(h_j + h_{j-1}) + 2t_s\delta_m) \\
&\quad + \sum_{j=1}^n E_j t_j \left(\frac{h_j^2 + h_j h_{j-1} + h_{j-1}^2}{3} - (h_j + h_{j-1})\delta_m + \delta_m^2 \right) \\
&\quad + \sum_{j=1}^m E_j t_j \left(\frac{h_j^2 + h_j h_{j-1} + h_{j-1}^2}{3} + (h_j + h_{j-1})\delta_m + \delta_m^2 \right)
\end{aligned}$$

The change of curvature can be calculated as:

$$\Delta\kappa_m = \frac{M_m}{S_m}$$

The force generated by the misfit strain can be computed as follows:

$$\begin{aligned}
\frac{F_m}{b} &= \frac{M_m}{b} (h_{m-1} + \delta_{m-1} + t_s + t_m/2)^{-1} \\
&= \frac{S_m}{b} \Delta\kappa_m (h_{m-1} + \delta_{m-1} + t_s + t_m/2)^{-1}
\end{aligned}$$

In order to calculate the stress distribution as a result of the misfit strain caused by the deposition of the m^{th} layer, a equivalent substrate and deposit thickness in the composite

beam is computed as follows:

$$t_{(s,n+m)} = \frac{E_s t_s + \sum_{j=1}^n E_j t_j + \sum_{j=1}^{m-1} E_j t_j}{E_s} \quad \text{and} \quad t_{(i,n+m)} = \frac{E_s t_s + \sum_{j=1}^n E_j t_j + \sum_{j=1}^{m-1} E_j t_j}{E_i}$$

where $t_{(s,n+m)}$ is the equivalent substrate thickness for the composite beam. Similarly, $t_{(i,n+m)}$ is the equivalent deposit thickness for the i^{th} layer in the composite beam, it includes the already deposited n layers.

Then, the stress distribution in the substrate after deposition m^{th} layer is:

$$\sigma_{(s,n+m)}(y) = \sigma_{(s,n)}(y) - \sum_{j=1}^m \frac{F_j}{b} (t_{(s,n+j)})^{-1} + E_s \Delta \kappa_j (y - \delta_j)$$

for $y \in [-t_s, 0]$, where $\sigma_{(s,n)}(y)$ is the same as calculated in Section 2.1.3.

Similarly, the stress distribution in the i^{th} layer can be calculated as:

$$\sigma_{(i,n+m)}(y) = \sigma_{(i,n)} - \sum_{j=i+1}^m \frac{F_j}{b} (t_{(i,n+j)})^{-1} + E_i \Delta \kappa_j (y - \delta_j)$$

for $y \in [h_{i-1}, h_i]$, where $\sigma_{(i,n)}(y)$ is the same as calculated in Section 2.1.3.

On the other hand, for $y \in [-h_k - t_s, -h_{k-1} - t_s]$ the stress distribution on the k^{th} layer on the other side of the substrate is:

$$\sigma_{(k,n+m)}(y) = \frac{F_k}{b} t_k^{-1} - E_k \Delta \kappa_k (y - \delta_k) - \sum_{j=k+1}^m \frac{F_j}{b} (t_{(k,n+j)})^{-1} + E_j \Delta \kappa_j (y - \delta_j)$$

2.2 Analytic Model for Thermal Stress (during deposition and post deposition)

In thermal spray, the substrate temperature is raised due to the torch heating. In most cases, the temperature reached is not constant and it presents variations (sometimes not negligible) as the torch moves depositing several layers. Due to torch rastering and free or forced cooling by convection these temperature gradients (specially the first onset of spraying session) induce a misfit strain due to CTE mismatch, which produces a thermal stress distribution through the beam thickness. This CTE misfit generates a curvature change $\Delta\kappa_T$ which depends on the temperature gradient during processing. Once the deposition is completed, the same effect occurs during cooling. A typical graph of a spraying session can be found on Figure 2.1.

during deposition some $\Delta\kappa$ responds to thermal stresses and not only due to intrinsic stresses. The goal here is to calculate that curvature portion and subtract it from the experimental data to obtain the exact $\delta\kappa$ that responds to intrinsic stresses.

2.2.1 Thermal Stresses of n layers on the substrate

The strain in the multilayer system can be decomposed into a uniform component due to thermal mismatch product of the tensile/compressive forces and a bending component (product of the bending moment). [13] It can be calculated as:

$$\varepsilon_n(y) = c_n - (y - \delta_n)\Delta\kappa_{(T,n)}$$

where c_n is the uniform strain component when the n^{th} layer is deposited due to thermal mismatch, δ_n is the neutral axis position for the composite beam, and $\Delta\kappa_{(T,n)}$ is the change in curvature due to temperature difference, when the beam has n layers of the coating.

As an equilibrium requirement, the resultant force due to the uniform strain component must be zero: [13]

$$E_s t_s (c_n - \alpha_s \Delta T_n) + \sum_{j=1}^n E_j t_j (c_n - \alpha_j \Delta T_n) = 0$$

Therefore, the uniform strain component is:

$$c_n = \frac{\left(E_s t_s \alpha_s + \sum_{j=1}^n E_j t_j \alpha_j \right) \Delta T_n}{E_s t_s + \sum_{j=1}^n E_j t_j}$$

The normal stress in the substrate and the coating are related to strains by: [13]

$$\begin{aligned} \sigma_{(s,n)}(y) &= E_s (\varepsilon_n - \alpha_s \Delta T_n), \quad y \in [0, t_s] \\ \sigma_{(i,n)}(y) &= E_i (\varepsilon_n - \alpha_i \Delta T_n), \quad y \in [h_{i-1}, h_i] \end{aligned}$$

where $\sigma_{(s,n)}$ is the stress distribution in the substrate, and $\sigma_{(i,n)}$ is the stress distribution in the i^{th} layer after the deposition/cooling stage of the n^{th} layer, respectively. Finally, the sum of the bending moment with respect to the bending axis is zero, [13] therefore:

$$\int_{-t_s}^{h_n} E_y (c_n - \alpha_y \Delta T_n - (y - \delta_n) \Delta \kappa_{(T,n)}) y dy = 0$$

Using this expression it is possible to obtain the change in curvature due to a temperature gradient, as follows:

$$\begin{aligned} & \int_{-t_s}^{h_n} E_y (c_n - \alpha_y \Delta T_n) y dy - \int_{-t_s}^{h_n} E_y (y - \delta_n) y \Delta \kappa_{(T,n)} dy = 0 \\ & \int_{-t_s}^0 E_s (c_n - \alpha_s \Delta T_n) y dy + \sum_{j=1}^n \int_{h_{j-1}}^{h_j} E_j (c_n - \alpha_j \Delta T_n) y dy \\ & - \int_{-t_s}^0 E_s (y - \delta_n) y \Delta \kappa_{(T,n)} dy - \sum_{j=1}^n \int_{h_{j-1}}^{h_j} E_j (y - \delta_n) y \Delta \kappa_{(T,n)} dy = 0 \end{aligned}$$

Therefore, the curvature change due to the temperature difference is:

$$\begin{aligned}
\Delta\kappa_{(T,n)} &= \frac{E_s(c_n - \alpha_s\Delta T_n) \int_{-t_s}^0 y \, dy + \sum_{j=1}^n E_j(c_n - \alpha_j\Delta T_n) \int_{h_{j-1}}^{h_j} y \, dy}{E_s \int_{-t_s}^0 y^2 - y\delta_n \, dy + \sum_{j=1}^n E_j \int_{h_{j-1}}^{h_j} y^2 - y\delta_n \, dy} \\
\Delta\kappa_{(T,n)} &= \frac{E_s(c_n - \alpha_s\Delta T_n) \frac{t_s(-t_s)}{2} + \sum_{j=1}^n E_j(c_n - \alpha_j\Delta T_n) \frac{t_j(h_j + h_{j-1})}{2}}{E_s \left(\frac{t_s(t_s^2)}{3} - \frac{t_s(-t_s)}{2} \delta_n \right) + \sum_{j=1}^n E_j \left(\frac{(t_j)(h_j^2 + h_j h_{j-1} + h_{j-1}^2)}{3} - \frac{(t_j)(h_j + h_{j-1})}{2} \delta_n \right)} \\
\Delta\kappa_{(T,n)} &= \frac{-E_s t_s^2 (c_n - \alpha_s \Delta T_n) / 2 + \sum_{j=1}^n E_j t_j (c_n - \alpha_j \Delta T_n) (2h_{j-1} + t_j) / 2}{E_s \left(\frac{t_s(t_s^2)}{3} - \frac{t_s(-t_s)}{2} \delta_n \right) + \sum_{j=1}^n E_j \left(\frac{(t_j)(h_j^2 + h_j h_{j-1} + h_{j-1}^2)}{3} - \frac{(t_j)(h_j + h_{j-1})}{2} \delta_n \right)} \\
\Delta\kappa_{(T,n)} &= \frac{3 \left(-E_s t_s^2 (c_n - \alpha_s \Delta T_n) + \sum_{j=1}^n E_j t_j (c_n - \alpha_j \Delta T_n) (2h_{j-1} + t_j) \right)}{E_s t_s^2 (2t_s + 3\delta_n) + \sum_{j=1}^n E_j t_j (2(h_j^2 + h_j h_{j-1} + h_{j-1}^2) - 3\delta_n (h_j + h_{j-1}))} \quad (2.7)
\end{aligned}$$

2.2.2 Thermal Stresses of m layers on the other side of the substrate

Similarly to Section 2.2.1, the resultant force due to the uniform strain component must be zero:

$$E_s t_s (c_m - \alpha_s \Delta T_m) + \sum_{j=1}^n E_j t_j (c_m - \alpha_j \Delta T_m) + \sum_{j=1}^m E_j t_j (c_m - \alpha_j \Delta T_m) = 0$$

Therefore, the uniform strain component is:

$$c_m = \frac{\left(E_s t_s \alpha_s + \sum_{j=1}^n E_j t_j \alpha_j + \sum_{j=1}^m E_j t_j \alpha_j \right) \Delta T_m}{E_s t_s + \sum_{j=1}^n E_j t_j + \sum_{j=1}^m E_j t_j} \quad (2.8)$$

The normal stresses in the substrate and the layers are related to strains by:

$$\begin{aligned} \sigma_{(s,n+m)}(y) &= E_s(\varepsilon_m - \alpha_s \Delta T_m), \quad y \in [0, t_s] \\ \sigma_{(i,n+m)}(y) &= E_i(\varepsilon_m - \alpha_i \Delta T_m), \quad y \in [-h_i - t_s, -h_{i-1} - t_s] \end{aligned}$$

where $\sigma_{(s,n+m)}(y)$ is the stress distribution in the substrate, and $\sigma_{(i,n+m)}$ is the stress distribution on the i^{th} layer after deposition of the m^{th} layer. Finally, the sum of the bending moment with respect to the bending axis is zero, [13] therefore:

$$\int_{-h_m - t_s}^{h_n} E_y (c_m - \alpha_y \Delta T_m - (y - \delta_m) \Delta \kappa_{(T,m)}) y dy = 0$$

Using this expression it is possible to obtain the change in curvature as follows:

$$\begin{aligned} & \int_{-h_m - t_s}^{h_n} E_y (c_m - \alpha_y \Delta T_m) y dy - \int_{-h_m - t_s}^{h_n} E_y (y - \delta_n) y \Delta \kappa_{(T,n)} dy = 0 \\ & \sum_{j=1}^m \int_{-h_j - t_s}^{-h_{j-1} - t_s} E_j (c_m - \alpha_j \Delta T_m) y dy + \int_{-t_s}^{h_n} E_y (c_m - \alpha_y \Delta T_m) y dy \\ & - \sum_{j=1}^m \int_{-h_j - t_s}^{-h_{j-1} - t_s} E_j (y - \delta_m) y \Delta \kappa_{(T,m)} dy - \int_{-t_s}^{h_n} E_y (y - \delta_m) y \Delta \kappa_{(T,m)} dy = 0 \end{aligned}$$

Therefore, the curvature change due to temperature difference is:

$$\begin{aligned}\Delta\kappa_{(T,m)} &= \frac{\sum_{j=1}^m E_j(c_m - \alpha_j \Delta T_m) \int_{-h_j - t_s}^{-h_{j-1} - t_s} y \, dy + \int_{-t_s}^{h_n} E_y(c_m - \alpha_y \Delta T_m) y \, dy}{\sum_{j=1}^m E_j \int_{-h_j - t_s}^{-h_{j-1} - t_s} y^2 - y \delta_m \, dy + \int_{-t_s}^{h_n} E_y(y - \delta_m) y \, dy} \\ \Delta\kappa_{(T,m)} &= \frac{\sum_{j=1}^m E_j(c_m - \alpha_j \Delta T_m) \frac{-t_j(h_j + h_{j-1} + 2t_s)}{2} + \int_{-t_s}^{h_n} E_y(c_m - \alpha_y \Delta T_m) y \, dy}{\sum_{j=1}^m E_j t_j \left(\frac{(h_j + t_s)^2 + (h_j + t_s)(h_{j-1} + t_s) + (h_{j-1} + t_s)^2}{3} + \frac{h_j + h_{j-1} + 2t_s}{2} \delta_m \right) + \int_{-t_s}^{h_n} E_y(y - \delta_m) y \, dy} \\ \Delta\kappa_{(T,m)} &= \frac{\int_{-t_s}^{h_n} E_y(c_m - \alpha_y \Delta T_m) y \, dy - \sum_{j=1}^m E_j t_j (c_m - \alpha_j \Delta T_m) \frac{2h_{j-1} + t_j}{2} - t_s \sum_{j=1}^m E_j t_j (c_m - \alpha_j \Delta T_m)}{\sum_{j=1}^m E_j t_j \left(\frac{h_j^2 + h_j h_{j-1} + h_{j-1}^2}{3} + t_s^2 + t_s(h_j + h_{j-1}) + \frac{h_j + h_{j-1} + 2t_s}{2} \delta_m \right) + \int_{-t_s}^{h_n} E_y(y - \delta_m) y \, dy} \quad (2.9)\end{aligned}$$

Remark 2.2. Recall from Section 2.2.1 that

$$\int_{-t_s}^{h_n} E_y(c_m - \alpha_y \Delta T_m) y \, dy = -E_s t_s^2 (c_m - \alpha_s \Delta T_m) + \sum_{j=1}^n E_j t_j (c_n - \alpha_j \Delta T_m) (2h_{j-1} + t_j)$$

If the same number of layers on both sides of the substrate is applied and each layer is made of the same material with the same thickness, the numerator in the curvature Equation 2.9 can be computed as:

$$\begin{aligned}\text{num} &= -E_s t_s^2 (c_m - \alpha_s \Delta T_m) / 2 + \sum_{j=1}^n E_j t_j (c_n - \alpha_j \Delta T_m) (2h_{j-1} + t_j) / 2 \\ &\quad - \sum_{j=1}^m E_j t_j (c_m - \alpha_j \Delta T_m) \frac{2h_{j-1} + t_j}{2} - t_s \sum_{j=1}^m E_j t_j (c_m - \alpha_j \Delta T_m) \\ \text{num} &= -E_s t_s^2 (c_m - \alpha_s \Delta T_m) / 2 - t_s E_d h_m (c_m - \alpha_d \Delta T_m)\end{aligned}$$

The uniform strain component can be simplified from Equation 2.8 as:

$$c_m = \frac{(E_s t_s \alpha_s + 2E_d h_m \alpha_d) \Delta T_m}{E_s t_s + 2E_d h_m}$$

Therefore:

$$c_m - \alpha_s \Delta T_m = 2E_d h_m \Delta T_m (\alpha_d - \alpha_s)$$

$$c_m - \alpha_d \Delta T_m = E_s t_s \Delta T_m (\alpha_s - \alpha_d)$$

Finally, note that:

$$\begin{aligned} \text{num} &= -E_s t_s^2 (2E_d h_m \Delta T_m (\alpha_d - \alpha_s)) / 2 - t_s E_d h_m (E_s t_s \Delta T_m (\alpha_s - \alpha_d)) \\ &= E_s t_s^2 E_d h_m \Delta T_m (\alpha_s - \alpha_d) - E_s t_s^2 E_d h_m \Delta T_m (\alpha_s - \alpha_d) \\ &= 0 \end{aligned}$$

Thus, the total curvature change from the beginning of the process until coatings are deposited in both side of the substrate is zero.

2.3 Final Stress Distribution

Since all this analytic analysis so far assumes a linear elastic behavior for the substrate and the coating, the superposition principle can be used to add the stresses developed in the deposition (intrinsic: quenching+penning, and thermal during deposition) and cooling (only thermal) stages.

For this section, the calculation is applied for a substrate coated with n layers in one side of the substrate.

2.3.1 Deposition Stage

The deposition process generates a residual stress distribution due to the quenching and peening effects and the CTE misfit. Since the stress distribution is linear for the substrate

(due to linearity assumptions) it suffices to calculate the top and bottom stresses, and then interpolate the values for points in the inside. Let $\sigma_s(1, n) = \sigma_{(s,n)}(0)$ as in Section 2.1.3; i.e the stress at the top part of the substrate after the n^{th} layer has been deposited. Similarly, let $\sigma_s(2, n) = \sigma_{(s,n)}(-t_s)$ as in Section 2.1.3; i.e the stress at the bottom part of the substrate after the n^{th} layer has been deposited.

For thermal stress distribution, recall from Section 2.2.1 that $\sigma_{(s,n)}(y)$ is the stress induced on the substrate by deposition of the n^{th} layer. Let $\sigma_{(s,T)}(1, n) = \sigma_{(s,n)}(0)$; i.e the stress at the top part of the substrate due to the n^{th} temperature gradient required to deposit the n^{th} layer. Similarly, let $\sigma_{(s,T)}(2, n) = \sigma_{(s,n)}(-t_s)$ be the stress at the bottom part of the substrate due to the n^{th} temperature gradient.

Let $\sigma_s(1)$ be the stress at the top part of the substrate ($y = 0$) at the end of the coating process, it can be calculated as follows:

$$\begin{aligned}\sigma_s(1) &= \sigma_s(1, n) + \sum_{j=1}^n \sigma_{(s,T)}(1, j) \\ \sigma_s(1) &= -\sum_{j=1}^n \left(\frac{F_j}{b} (t_{(s,j)})^{-1} - E_s \Delta \kappa_j \delta_j \right) + \sum_{j=1}^n E_s (c_j - \alpha_s \Delta T_j + \delta_j \Delta \kappa_{(T,j)})\end{aligned}$$

Let $\sigma_s(2)$ be the stress at the bottom part of the substrate ($y = -t_s$) at the end of the coating process, it can be calculated as follows:

$$\begin{aligned}\sigma_s(2) &= \sigma_s(2, n) + \sum_{j=1}^n \sigma_{(s,T)}(2, j) \\ \sigma_s(2) &= -\sum_{j=1}^n \left(\frac{F_j}{b} (t_{(s,j)})^{-1} - E_s \Delta \kappa_j (t_s + \delta_j) \right) + \sum_{j=1}^n E_s (c_j - \alpha_s \Delta T_j + (t_s + \delta_j) \Delta \kappa_{(T,j)})\end{aligned}$$

For the stress distribution on the coatings layers, the stress of the middle point of each layer is determined. Since the thickness of the layers are relatively small in comparison with the thickness of the substrate, the middle point stress can be taken as an approximated average

of the stress distribution on that specific layer. For the i^{th} layer, the midpoint is located in $y = h_i - t_i/2$. Let $\sigma_d(i, n) = \sigma_{(i,n)}(h_i - t_i/2)$ as in Section 2.1.3; i.e the stress at the midpoint of i^{th} layer after the n^{th} layer has been deposited.

For thermal stress distribution on the deposit, recall from Section 2.2.1 that $\sigma_{(i,n)}(y)$ is the stress induced on the i^{th} layer by deposition of the n^{th} layer. Let $\sigma_{(d,T)}(i, n) = \sigma_{(i,n)}(h_i - t_i/2)$; i.e the stress at midpoint of the i^{th} layer due to the n^{th} temperature gradient required to deposit the n^{th} layer.

Let $\sigma_d(i)$ be the stress at the midpoint of the i^{th} layer ($y = h_i - t_i/2$) at the end of the coating process, it can be calculated as follows:

$$\begin{aligned}\sigma_d(i) &= \sigma_s(i, n) + \sum_{j=1}^n \sigma_{(s,T)}(i, j) \\ \sigma_d(i) &= \frac{F_i}{b} t_i^{-1} - E_i \Delta \kappa_i (h_i - t_i/2 - \delta_i) - \sum_{j=i+1}^n \left(\frac{F_j}{b} (t_{(i,j)})^{-1} + E_i \Delta \kappa_j (h_i - t_i/2 - \delta_j) \right) \\ &\quad + \sum_{j=1}^n E_i (c_j - \alpha_s \Delta T_j - (h_i - t_i/2 - \delta_j) \Delta \kappa_{(T,j)})\end{aligned}$$

2.3.2 Cooling stage: post spraying

After the n layers have been deposited on the substrate, the composite beam will cool down until it reaches room temperature. In this case, thermal stress is developed by a temperature gradient ΔT_c . This gradient induces a change in curvature $\Delta \kappa_c$. Subindex c corresponds to cooling.

Let $\sigma_{(s,T_c)}(1, n)$ the the stress at the top part of the substrate due to the cooling process after deposition of the n^{th} layer, and let $\sigma_{(d,T_c)}(i, n)$ be the stress at the midpoint of the layer i once it is cooled down after deposition of the n^{th} layer.

Let $\sigma_{(s,c)}(1)$ be the stress at the top part of the substrate ($y = 0$) at the end of the cooling process, it can be calculated as follows:

$$\begin{aligned}\sigma_{(s,c)}(1) &= \sigma_{(s,T_c)}(1, n) \\ \sigma_{(s,c)}(1) &= E_s (c_n - \alpha_s \Delta T_c + \delta_n \Delta \kappa_c)\end{aligned}$$

Let $\sigma_{(s,c)}(2)$ be the stress at the bottom part of the substrate ($y = -t_s$) at the end of the cooling process, it can be calculated as follows:

$$\begin{aligned}\sigma_{(s,c)}(2) &= \sigma_{(s,T)}(2, j) \\ \sigma_{(s,c)}(2) &= E_s (c_n - \alpha_s \Delta T_c + (t_s + \delta_n) \Delta \kappa_c)\end{aligned}$$

For the coating layers, Let $\sigma_{(d,c)}(i)$ be the stress at the midpoint of the i^{th} layer ($y = h_i - t_i/2$) at the end of the cooling process, it can be calculated as follows:

$$\begin{aligned}\sigma_{(d,c)}(i) &= \sigma_{(d,T_c)}(i, n) \\ \sigma_{(d,c)}(i) &= E_i (c_n - \alpha_i \Delta T_c - (h_i - t_i/2 - \delta_n) \Delta \kappa_c)\end{aligned}$$

2.4 Multilayer model of a coating of a single material

Suppose that the same material is deposited over a substrate in n different layers. All coating layers can be assumed identical as they are deposited continuously and using a robotic arm. The following section shows a simplified version of the equations stated in Sections 2.1.3 and 2.2.1 when the modulus of each layer can be generalized for a single material, where: $E_i = E_d \quad \forall i \in \{1, \dots, n\}$ and $t_i = t_d \quad \forall i \in \{1, \dots, n\}$. Recall that $h_n = \sum t_j = n(t_d)$. For proofs of summation identities refer to Appendix A.

The neutral axis position is:

$$\begin{aligned}
\delta_n &= \frac{-E_s t_s^2 + \sum_{j=1}^n E_j t_j (2h_{j-1} + t_j)}{2 \left(E_s t_s + \sum_{j=1}^n E_j t_j \right)} \\
&= \frac{-E_s t_s^2 + E_d t_d^2 \sum_{j=1}^n (2(j-1) + 1)}{2 \left(E_s t_s + E_d t_d \sum_{j=1}^n 1 \right)} \\
&= \frac{-E_s t_s^2 + E_d t_d^2 \sum_{j=1}^n (2j-1)}{2(E_s t_s + E_d t_d (n))} \\
\delta_n &= \frac{-E_s t_s^2 + E_d (n t_d)^2}{2(E_s t_s + E_d (n t_d))}
\end{aligned}$$

The composite beam stiffness is:

$$\begin{aligned}
\frac{S_n}{b} &= E_s t_s \left(\frac{t_s^2}{3} + t_s \delta_n + \delta_n^2 \right) + \sum_{j=1}^n E_j t_j \left(\frac{h_j^2 + h_j h_{j-1} + h_{j-1}^2}{3} - (h_j + h_{j-1}) \delta_n + \delta_n^2 \right) \\
&= E_s t_s \left(\frac{t_s^2}{3} + t_s \delta_n + \delta_n^2 \right) + E_d t_d \sum_{j=1}^n \left(\frac{t_d^2}{3} (j^2 + j(j-1) + (j-1)^2) - t_d (j + j-1) \delta_n + \delta_n^2 \right) \\
&= E_s t_s \left(\frac{t_s^2}{3} + t_s \delta_n + \delta_n^2 \right) + E_d t_d \left(\frac{t_d^2}{3} \sum_{j=1}^n (3j^2 - 3j + 1) - t_d \sum_{j=1}^n (2j-1) \delta_n + \sum_{j=1}^n \delta_n^2 \right) \\
\frac{S_n}{b} &= E_s t_s \left(\frac{t_s^2}{3} + t_s \delta_n + \delta_n^2 \right) + E_d (n t_d) \left(\frac{(n t_d)^2}{3} - (n t_d) \delta_n + \delta_n^2 \right)
\end{aligned}$$

The force is:

$$\begin{aligned}
\frac{F_n}{b} &= \frac{S_n}{b} \Delta \kappa_n (h_{n-1} - \delta_{n-1} + t_n/2)^{-1} \\
\frac{F_n}{b} &= \frac{S_n}{b} \Delta \kappa_n (t_d (n-1) - \delta_{n-1} + t_d/2)^{-1}
\end{aligned}$$

The equivalent thickness is:

$$t_{(s,n)} = \frac{E_s t_s + \sum_{j=1}^{n-1} E_j t_j}{E_s} \quad \text{and} \quad t_{(i,n)} = \frac{E_s t_s + \sum_{j=1}^{n-1} E_j t_j}{E_i}$$

$$t_{(s,n)} = \frac{E_s t_s + E_d (n t_d)}{E_s} \quad \text{and} \quad t_{(i,n)} = \frac{E_s t_s + E_d (n t_d)}{E_i}$$

The uniform strain component is:

$$c_n = \frac{\left(E_s t_s \alpha_s + \sum_{j=1}^n E_j t_j \alpha_j \right) \Delta T}{E_s t_s + \sum_{j=1}^n E_j t_j}$$

$$c_n = \frac{(E_s t_s \alpha_s + E_d (n t_d) \alpha_d) \Delta T_n}{E_s t_s + E_d (n t_d)}$$

The curvature change due to temperature difference is:

$$\Delta \kappa_{(T,n)} = \frac{3 \left(-E_s t_s^2 (c_n - \alpha_s \Delta T_n) + \sum_{j=1}^n E_j t_j (c_n - \alpha_j \Delta T_n) (2h_{j-1} + t_j) \right)}{E_s t_s^2 (2t_s + 3\delta_n) + \sum_{j=1}^n E_j t_j (2(h_j^2 + h_j h_{j-1} + h_{j-1}^2) - 3\delta_n (h_j + h_{j-1}))}$$

$$= \frac{3 \left(-E_s t_s^2 (c_n - \alpha_s \Delta T_n) + E_d t_d (c_n - \alpha_d \Delta T_n) \sum_{j=1}^n t_d (2(j-1) + 1) \right)}{E_s t_s^2 (2t_s + 3\delta_n) + E_d t_d \sum_{j=1}^n 2t_d^2 (j^2 + j(j-1) + (j-1)^2) - 3t_d \delta_n (j + j - 1)}$$

$$= \frac{3 \left(-E_s t_s^2 (c_n - \alpha_s \Delta T_n) + E_d t_d^2 (c_n - \alpha_d \Delta T_n) \sum_{j=1}^n 2j - 1 \right)}{E_s t_s^2 (2t_s + 3\delta_n) + E_d t_d^2 \left(2t_d \sum_{j=1}^n (3j^2 - 3j + 1) - 3\delta_n \sum_{j=1}^n 2j - 1 \right)}$$

$$\begin{aligned}
&= \frac{3(-E_s t_s^2 (c_n - \alpha_s \Delta T_n) + E_d (nt_d)^2 (c_n - \alpha_d \Delta T_n))}{E_s t_s^2 (2t_s + 3\delta_n) + E_d (nt_d)^2 (2(nt_d) - 3\delta_n)} \\
&= \frac{3\left(-E_s t_s^2 \left(\frac{E_d (nt_d)(\alpha_d - \alpha_s) \Delta T_n}{E_s t_s + E_d (nt_d)}\right) + E_d (nt_d)^2 \left(\frac{E_s t_s (\alpha_s - \alpha_d) \Delta T_n}{E_s t_s + E_d (nt_d)}\right)\right)}{2E_s t_s^3 + 3E_s t_s^2 \frac{-E_s t_s^2 + E_d (nt_d)^2}{2(E_s t_s + E_d (nt_d))} + 2E_d (nt_d)^3 - 3E_d (nt_d)^2 \frac{-E_s t_s^2 + E_d (nt_d)^2}{2(E_s t_s + E_d (nt_d))}} \\
&= \frac{6(E_s t_s^2 E_d (nt_d)(\alpha_s - \alpha_d) \Delta T_n + E_d (nt_d)^2 E_s t_s (\alpha_s - \alpha_d) \Delta T_n)}{4E_s^2 t_s^4 + 4E_s t_s^3 E_d (nt_d) + 4E_s t_s E_d (nt_d)^3 + 4E_d^2 h^4 - 3E_s^2 t_s^4 + 6E_s t_s^2 E_d (nt_d)^2 - 3E_d^2 (nt_d)^4} \\
\Delta \kappa_{(T,n)} &= \frac{6E_s t_s E_d (nt_d)(t_s + nt_d)(\alpha_s - \alpha_d) \Delta T_n}{E_s^2 t_s^4 + 4E_s t_s^3 E_d (nt_d) + 6E_s t_s^2 E_d (nt_d)^2 + 4E_s t_s E_d (nt_d)^3 + E_d^2 (nt_d)^4}
\end{aligned}$$

The stress distribution determined during the deposition stage is:

$$\begin{aligned}
\sigma_s(1) &= -\sum_{j=1}^n \left(\frac{F_j}{b} (t_{(s,j)})^{-1} - E_s \Delta \kappa_j \delta_j \right) + \sum_{j=1}^n E_s (c_j - \alpha_s \Delta T_j + \delta_j \Delta \kappa_{(T,j)}) \\
\sigma_s(2) &= -\sum_{j=1}^n \left(\frac{F_j}{b} (t_{(s,j)})^{-1} - E_s \Delta \kappa_j (t_s + \delta_j) \right) + \sum_{j=1}^n E_s (c_j - \alpha_s \Delta T_j + (t_s + \delta_j) \Delta \kappa_{(T,j)}) \\
\sigma_d(i) &= \frac{F_i}{b} t_d^{-1} - E_d \Delta \kappa_i (t_d(i - 1/2) - \delta_i) - \sum_{j=i+1}^n \left(\frac{F_j}{b} (t_{(i,j)})^{-1} + E_d \Delta \kappa_j (t_d(i - 1/2) - \delta_j) \right) \\
&\quad + \sum_{j=1}^n E_d (c_j - \alpha_s \Delta T_j - (t_d(i - 1/2) - \delta_j) \Delta \kappa_{(T,j)})
\end{aligned}$$

The stress distribution in cooling stage after deposition is:

$$\begin{aligned}
\sigma_{(s,c)}(1) &= E_s (c_n - \alpha_s \Delta T_c + \delta_n \Delta \kappa_c) \\
\sigma_{(s,c)}(2) &= E_s (c_n - \alpha_s \Delta T_c + (t_s + \delta_n) \Delta \kappa_c) \\
\sigma_{(d,c)}(i) &= E_d (c_n - \alpha_d \Delta T_c - (t_d(i - 1/2) - \delta_n) \Delta \kappa_c)
\end{aligned}$$

2.5 Application: Prediction of intrinsic stresses in bulky parts based on curvature experiment

Consider coating processes in which the substrate is stiff and thick enough to resist changes in curvature; i.e the curvature change after every deposition is negligible. In such case there is no need to measure the change in curvature. Nevertheless, the curvature method can still be applied to calculate the stress distribution in the following way:

1. Calculate the intrinsic stress using the curvature method for a experiment in which the same substrate and the coating material are used.
2. Use the intrinsic stress as an input (instead of the curvature) for the bulky part in order to calculate the force generated during the process.
3. Neglect the stress due to the curvature change and calculate only the one generated by the normal force.

Neglecting the stress caused by the curvature in equations described in Section 2.3, the final stress distribution is:

$$\begin{aligned}\sigma_s(1) &= -\sum_{j=1}^n \frac{F_j}{b} (t_{(s,j)})^{-1} + \sum_{j=1}^n E_s (c_j - \alpha_s \Delta T_j) \\ \sigma_s(2) &= -\sum_{j=1}^n \frac{F_j}{b} (t_{(s,j)})^{-1} + \sum_{j=1}^n E_s (c_j - \alpha_s \Delta T_j) \\ \sigma_d(i) &= \frac{F_i}{b} t_i^{-1} - \sum_{j=i+1}^n \frac{F_j}{b} (t_{(i,j)})^{-1} + \sum_{j=1}^n E_j (c_j - \alpha_s \Delta T_j)\end{aligned}$$

First of all, note that the stress distribution in the substrate is constant and the stress distribution in the entire i^{th} layer is constant too. Recall that the force F_i is generated due to quenching and peening misfit; therefore, even though there is no curvature in the system there is a misfit strain that causes a tensile/compressive force to the layers and the substrate.

Considering the linear elastic case, each new layer has to agree with the stress-strain equation $\sigma_q = \Delta\varepsilon E_d$ where σ_q is the intrinsic stress and $\Delta\varepsilon$ is the misfit strain. [12]

2.5.1 Deposition of the first layer

Consider the coating process showed in Figure 2.6. The misfit strain generates a pair of equal and opposite forces acting on the substrate and the first layer, each one generates a strain ε_s and ε_d respectively.

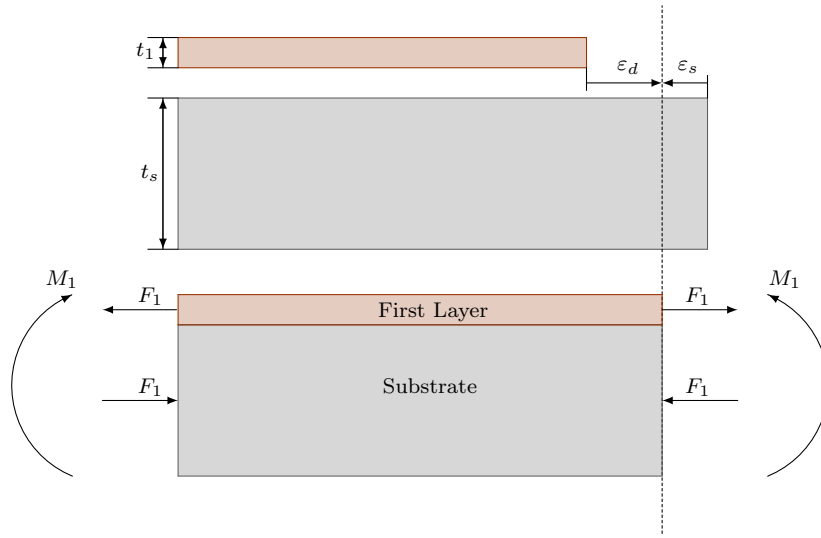


FIGURE 2.6: Normal strain generated in deposition of the first layer

Thus, the strain compatibility equation is:

$$\begin{aligned} \Delta\varepsilon_1 &= \varepsilon_d - \varepsilon_s \\ &= \frac{F_1}{bt_1 E_1} + \frac{F_1}{bt_s E_s} \\ &= \frac{\sigma_{(q,1)}}{E_1} \end{aligned}$$

Therefore, the value of the intrinsic stress can be calculated as follows:

$$\sigma_{(q,1)} = E_1 \frac{F_1}{b} \left(\frac{1}{E_s t_s} + \frac{1}{E_1 t_1} \right)$$

2.5.2 Deposition of the second layer

Similarly, the deposition of the second layer generates a misfit strain $\Delta\varepsilon_2$ which causes a pair of normal forces acting on both, the composite beam (substrate + first layer) and the second layer. Thus, the strain compatibility equation is:

$$\begin{aligned} \Delta\varepsilon_2 &= \varepsilon_d - \varepsilon_s \\ &= \frac{F_2}{bt_2 E_2} + \frac{F_2}{b(t_s + t_1) E_{(s,2)}} \\ &= \frac{\sigma_{(q,2)}}{E_2} \end{aligned}$$

Where $E_{(s,2)}$ is the equivalent Young's modulus for the composite beam.

$$E_{(s,2)} = \frac{E_s t_s + E_1 t_1}{t_s + t_1}$$

Therefore, the value of the quenching stress can be computed as follows:

$$\sigma_{(q,2)} = E_2 \frac{F_2}{b} \left(\frac{1}{E_s t_s + E_1 t_1} + \frac{1}{E_2 t_2} \right)$$

2.5.3 Deposition of the n^{th} layer

Finally, after the deposition of the n^{th} layer the strain compatibility equation is:

$$\begin{aligned}\Delta\varepsilon_n &= \varepsilon_d - \varepsilon_s \\ &= \frac{F_n}{bt_n E_n} + \frac{F_n}{b(t_s + h_{n-1})E_{(s,n)}} \\ &= \frac{\sigma_{(q,n)}}{E_n}\end{aligned}$$

Where $E_{(s,n)}$ is the equivalent Young's modulus for the composite beam.

$$E_{(s,n)} = \frac{E_s t_s + \sum_{j=1}^{n-1} E_j t_j}{t_s + h_{n-1}}$$

Therefore, the value of the intrinsic stress can be calculated as follows:

$$\sigma_{(q,n)} = E_n \frac{F_n}{b} \left(\frac{1}{E_s t_s + \sum_{j=1}^{n-1} E_j t_j} + \frac{1}{E_n t_n} \right)$$

2.5.4 Deposition of m layers on the other side of the substrate

Following the same logic, the quenching stress developed on the m^{th} layer on the other side of the substrate will be calculated as follows:

$$\sigma_{(q,n+m)} = E_m \frac{F_m}{b} \left(\frac{1}{E_s t_s + \sum_{j=1}^n E_j t_j + \sum_{j=1}^{m-1} E_j t_j} + \frac{1}{E_m t_m} \right)$$

2.5.5 Final stress distribution

This method can only be used if the experimental deposition system agrees with the real deposition system; in other words, the substrate material and the coating material have to be the same for both processes and they have to be deposited using the same techniques in both scenarios.

Experimentally it is possible to predict $\sigma_{(q,n)}$ using the equations stated above. To apply this analysis to a problem where the change of curvature is negligible, the intrinsic stress is determined from the curvature method. Then the normal force acting on each layer is calculated. Therefore, using the experimental values of $\sigma_{(q,n)}$ the force per width is determined as follows:

$$\frac{F_n}{b} = \frac{\sigma_{(q,n)}}{E_n} \left(\frac{1}{E_s t_s + \sum_{j=1}^{n-1} E_j t_j} + \frac{1}{E_n t_n} \right)^{-1}$$

Finally, this value is replaced in equations stated at the beginning of this section in order to get the stress distribution of the coating process.

For an example of this application refer to Section 3.6.1.

Chapter 3

Computer Model

The program presented in this section is an automatic stress distribution solver for a linear elastic multilayer deposition system, taking in consideration deposition and cooling stages and using as input data curvature and temperature measurements during the coating processing (*in-situ*). In the program, it is possible to divide the whole process in several deposition cycles. Each deposition cycle is constituted by a continuous deposition stage and a continuous cooling stage. It is assumed that a robotic arm will be used for the deposition process. In consequence, the thickness of each layer in a deposition cycle is assumed to be uniform. Figure 3.1 shows how the stages are divided in the process.

The necessity of an automatic program is due to the complexity of the stress distribution that can be developed in the deposit layers. Although the stress distribution is linear in the substrate, it is not necessarily linear in the coating (note that the distribution is linear in each layer, but not in the whole coating). In this study only the stress corresponding to the middle point of each layer is taken into count in order to predict how the stress distribution results in the composite beam. Figure 3.2 shows a possible scenario for the final stress distribution in a particular deposition process.

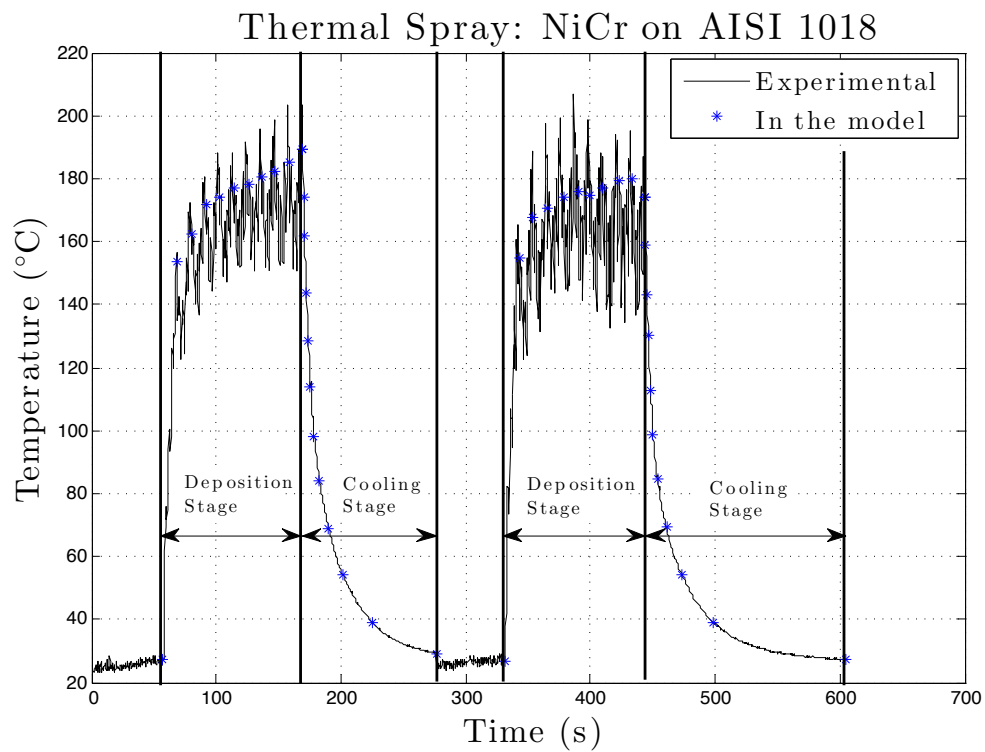


FIGURE 3.1: Description of deposition cycles used by the program

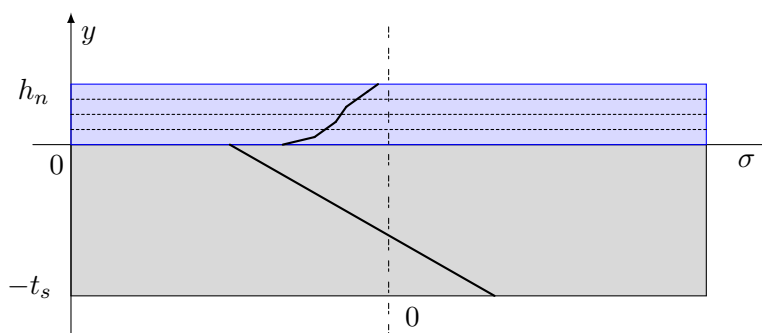


FIGURE 3.2: Schematic description of stress distribution through the thickness of the coating-substrate system

The software implemented in MATLAB[®] based on the analytic model presented in this study fulfills the following goals (as of Version 2.0):

- Calculates residual stresses and thermal stresses as a result of the coating processing.
- Allows for data acquisition and selection for further calculations.
- Solves multilayer system of various materials divided by several deposition cycles.
- Generate user-friendly results and graphics.
- Integration of curvature/temperature data produced by sensors (e.g. ICP-in-situ coating property sensor).

3.1 Data Acquisition

The curvature method applied to the measurements of the evolution of residual stress in thermal spray coatings requires acquisition of two variables: *Temperature* and *Curvature*. These variables allow to calculate the stress distribution from linear elastic mechanics with few assumptions and the feed of few parameters. Laser sensors and thermocouples set on the back of the substrate retrieve data during the thermal spraying. This data can be read by the program as an array. Each new layer contributes with a new pair of data (κ, T) .

Tsui and Clyne in their paper [12] describe the logic of a computer program used to solve the multilayer deposition of a single coating material, which was developed in Section 2.4. It is noteworthy the the authors use the quenching stress as an input to the program and they calculate the curvature using that information. Whereas in this study, the curvature data is fed in the program to calculate the stress and every process effect in thermal stresses is also taken into account. Table 3.1 compares the input data required for both models.

	Tsui-Clyne [12]	Multilayer [present study]
Mechanical Properties	Elastic Modulus (E_s)	Elastic Modulus (E_s)
	Poisson Ratio (ν_s)	Poisson Ratio (ν_s)
Substrate	CTE (α_s)	CTE (α_s)
Mechanical Properties	Elastic Modulus (E_d)	Elastic Modulus (E_d)
	Poisson Ratio (ν_d)	Poisson Ratio (ν_d)
Deposit	CTE (α_d)	CTE (α_d)
	Specimen Width (b)	
Dimensions	Substrate Thickness (H)	Substrate Thickness (t_s)
	Layer Thickness (w)	Layer Thickness (t_d)
Main Input parameters/ data	Quenching Stress (σ_q)	Curvature change ($\Delta\kappa$)
	Cooling Temperature (T_c)	Instantaneous temperature (T)
	Number of Layers (n)	Number of Layers (n)
Deposition session	One	As necessary

TABLE 3.1: Input data comparison between Tsui-Clyne model and multilayer analytic linear elastic model

Appendix C shows how data can be read from an external database. Every coating material has its deposition session and each one has its deposition and cooling stages. Every coating material has its own data set. In the example in Appendix C there is only one coating material, for this reason there is only one set of variables (Time, Temperature, and Curvature). Once the data is read from the external file it is filtered depending of how exact the measures of the set of variables is needed. In the example he have chosen to take data every 0.25 seconds.

The last step in data acquisition is to define which points represent better the deposition and cooling process as the data itself is produced with some noise. The user has to choose the time coordinate at which one layer starts being deposited and one where the deposition of that layer is finished. In the example, as we have two deposition sessions the set points of interest: `time_h11`, `temp_h11`, `kappa_h11` to represent the first deposition session (0.4 mm of NiCr coating on Steel) and the set of points of interest `time_h12`, `temp_h12`, `kappa_h12` to represent the second deposition session (another 0.4 mm of NiCr coating). For the points

of interest at the cooling stage it is necessary to determine the start and the end points for this stage, and decide the number of data points desired from this stage. In the example, the data from the cooling stages is taken every 15 degrees Celsius.

Figure 3.3 shows how data is read from the curvature-temperature file. In this case, the black line represents the data once filtered out (simply reducing the number of points as data input) and the blue asterisks represent the points of interest chosen by the user. Note that since there were deposited 10 layers in each deposition cycle there are 11 points of interest in each deposition stage.

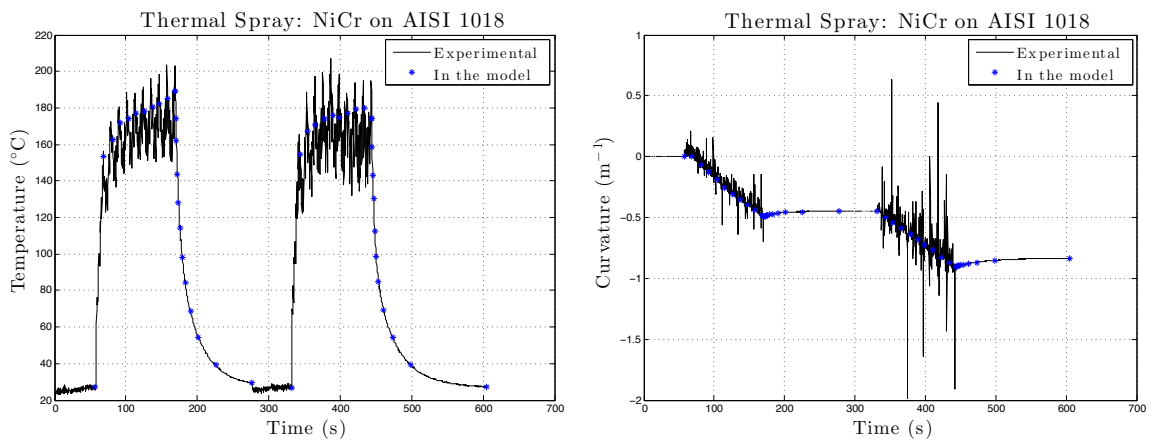


FIGURE 3.3: Points of interest used as input for calculations

3.2 Thermal Stress during deposition routine

Because of the thermal gradient during processing, some thermal stress during deposition occurs due to CTE mismatch. The curvature produced by the composite beam due to the thermal gradient generated by the heat input of a deposited layer can be calculated. The temperature gradient ΔT_i corresponding to the deposition of the i^{th} layer is the difference of the values T_{i-1} and T_i acquired in the reading routine. Note that only temperature data is needed, Figure 3.4 shows the temperature gradient they produces the thermal stresses during

deposition. Appendix E shows how this routine calculates thermal stresses and curvature variation ($\Delta\kappa_T$) at the end of every layer application.

3.3 Evolving Stress routine

For this calculation; curvature data is required from the data acquisition routine, and from the thermal stress during deposition routine. The curvature change $\Delta\kappa_i$ corresponding to the deposition of the i^{th} layer is the difference of the values κ_{i-1} and κ_i acquired in the reading routine minus the curvature change due to thermal stress (calculated in Equation 2.7). The curvature data recorded by the lasers correspond to both thermal and intrinsic stresses. Therefore, the curvature calculated in the thermal stress during deposition routine for each layer is subtracted from the one acquired from the lasers, i.e $\Delta\kappa = \Delta\kappa_{\text{recorded}} - \Delta\kappa_T$, Figure 3.4 shows how total curvature change is calculated. Appendix F describes this calculation. The final result is the residual stress distribution in the substrate and the deposit in each layer applied due to the quenching and peening, which in this paper is defined as evolving stress.

3.4 Intrinsic Stress routine

As pointed in Section 2.5, quenching stress (or evolving stress in a more general description) has to be calculated in the experimental model in order to be capable of calculate stress distribution in a real engineering problem where curvature change is negligible. In addition to this method, Stoney's approximation is also calculated in order to compare the exact method proposed in this study with the approximation given buy the following equation: [14]

$$\sigma_{SF} = \frac{E_s t_s^2}{6} \frac{\Delta\kappa}{\Delta t_d}$$

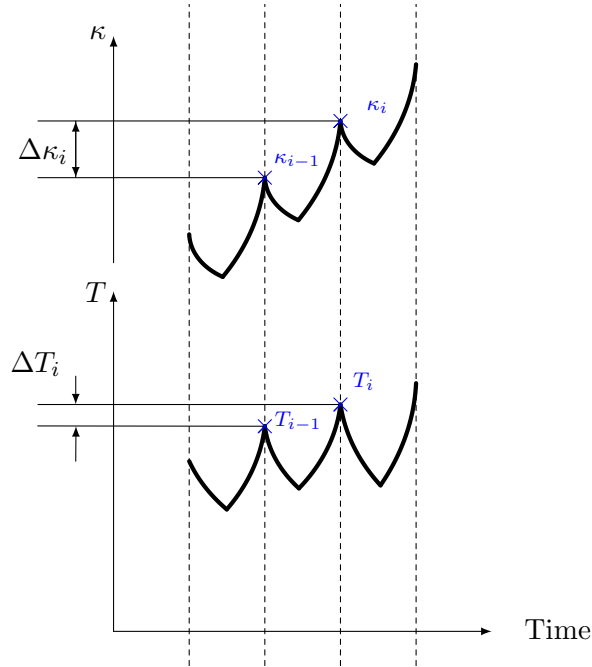


FIGURE 3.4: Data acquired in deposition

Where σ_{SF} is the average stress due to the deposition coating in the layer of thickness Δt_d , E_s is the effective Young modulus for the substrate, t_s is the substrate thickness, and $\Delta\kappa$ is the curvature change due to the deposition. Recall that the main assumption of Stoney formula is that the coating layer is much less thicker than the substrate. Appendix G shows the calculation of both linear elastic model and approximated intrinsic stress.

3.5 Thermal Stress during cooling post-deposition routine

Appendix D shows the logic for calculating the stress distribution in the cooling stage. Every two consecutive data pair (κ_{i-1}, T_{i-1}) and (κ_i, T_i) determines an interval i whose data pair associated is $(\Delta\kappa_i, \Delta T_i)$. Using the program, the output generated is the stress $\sigma_{(d,c)}(i)$ (as in Section 2.3.2). Figure 3.3 shows how the intervals are taken for calculations.

3.6 Results

Stress distribution at the end of the process is shown as a plot of stress as a function of the thickness position. Appendix H shows how the figures are constituted. As an example, the deposition process of NiCr over AISI 1018 steel is presented. HVOF has been used for the deposition and two deposition sessions have been accomplished. Each deposition cycle counts with a 10-layer continuous deposition stage and a cooling stage. As shown in Figure 3.3, there will be 11 points of interest for each deposition stage and the number of points of interest for the cooling stage varies according to how much the temperature drops. Appendix B shows the Main window in which the user has to establish the process parameters. Table 3.2 summarizes properties and parameters used for calculations. In Chapter 4, the method of calculating the elastic modulus and CTE for the deposit is discussed.

	Mechanical Properties			Thickness [mm]	Number of Passes
	E [GPa]	α [10^{-6}K^{-1}]	ν		
Substrate	200	12.2	0.29	2.431	—
Deposit	140	14.0	0.30	0.893	20

TABLE 3.2: Parameters used in deposition of NiCr on AISI1018

The final step is the plotting routine and it takes all the three different stress values calculated before (thermal stress during deposition, evolving stress, and thermal stress during cooling) and adds them together in order to calculate the final stress distribution. The result is presented in Figure 3.5.

This routine also provides a comparison between the intrinsic stress calculated and the Stoney formula approximation as shown in Figure 3.6.

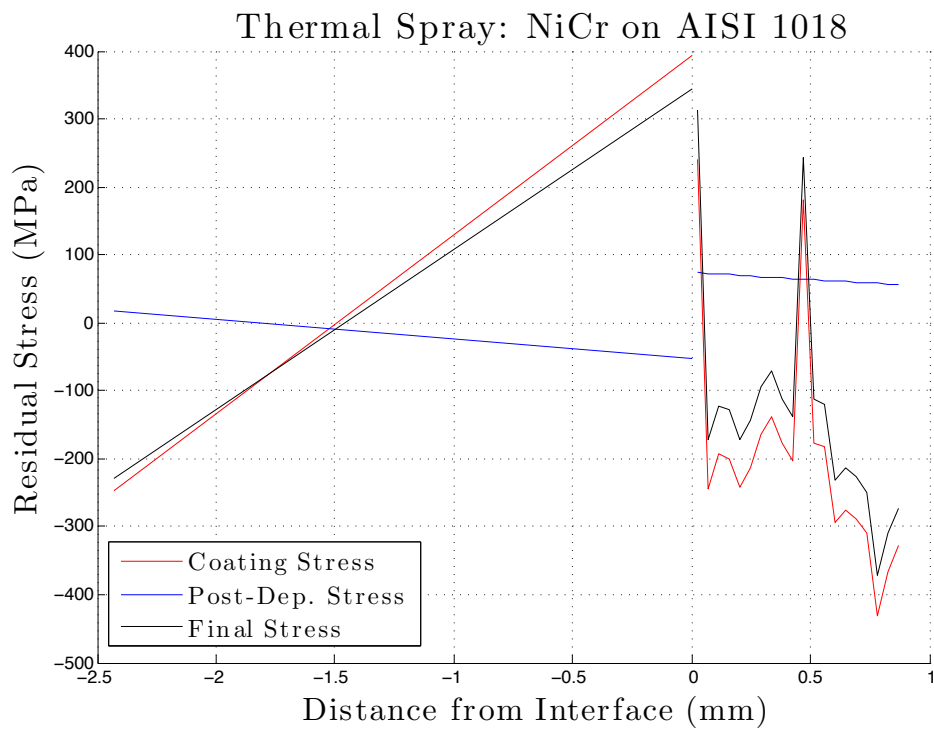


FIGURE 3.5: Final stress distribution in thermal spray NiCr on AISI 1018

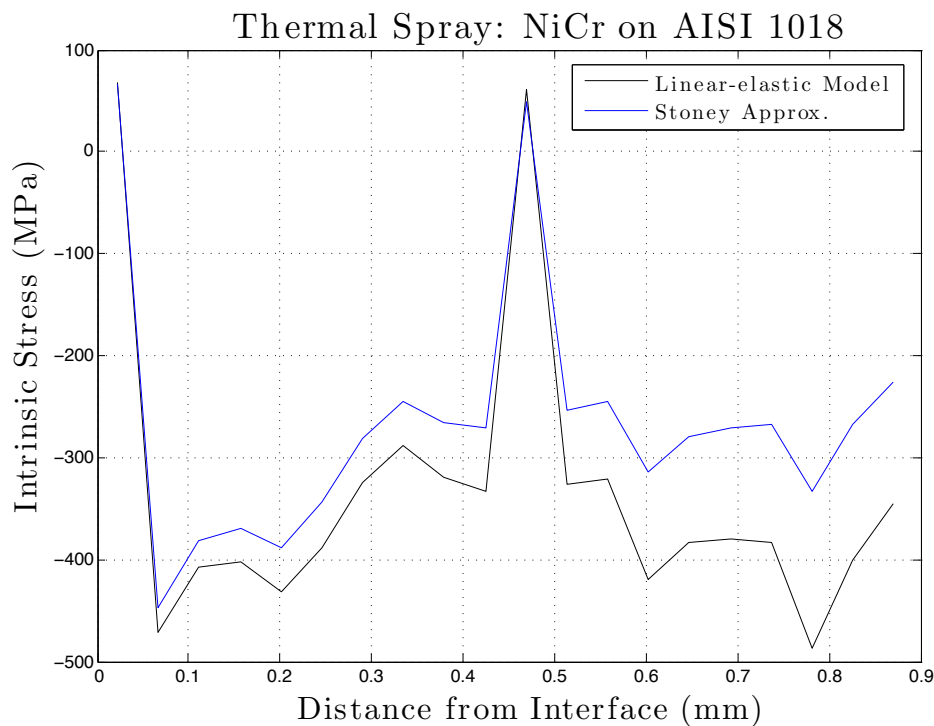


FIGURE 3.6: Comparison between analytic linear elastic model and Stoney formula (NiCr)

3.6.1 Prediction for bulky parts

Suppose that the same deposition process described above is used on a much thicker substrate. The same 20 layers of NiCr will be deposited on AISI1018 which thickness is 25 mm. In this case, assumptions made in Section 2.5 are met. Therefore, using the intrinsic stress distribution described in Figure 3.6 it is possible to predict the stress distribution resulting after the same deposition process on the bulky part.

Figure 3.7 shows the residual stress distribution calculated using equations in Section 2.5 and the intrinsic stress distribution shown in Figure 3.6. It is assumed that the curvature-temperature data is the same as in Figure 3.3.

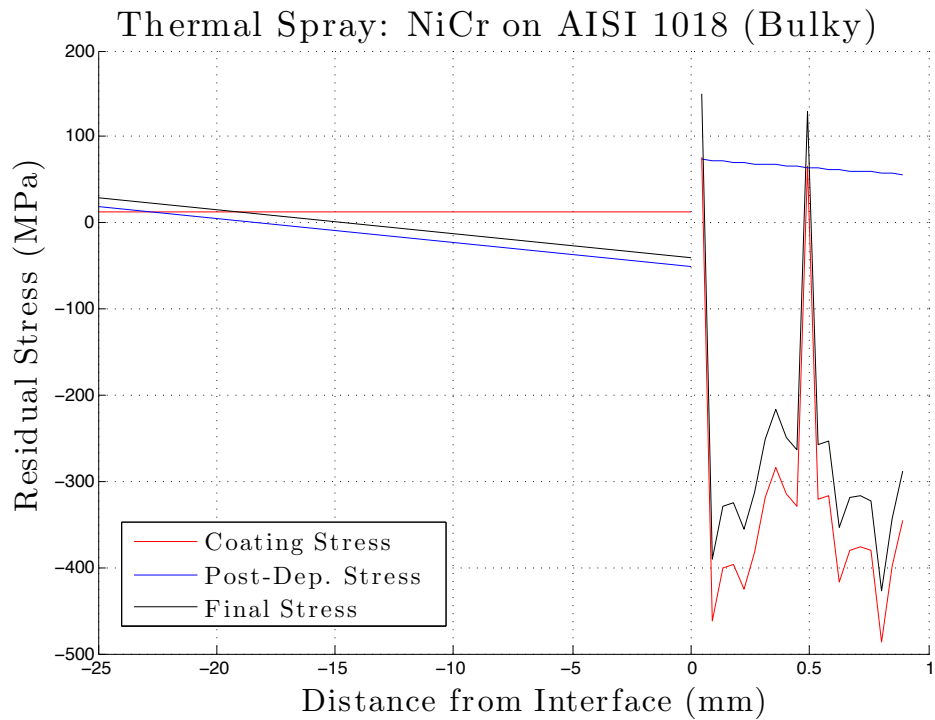


FIGURE 3.7: Final stress distribution in thermal spray NiCr on AISI 1018 (bulky)

3.6.2 Multilayer system with two different coating materials

As an example for a multilayer system where more two coating materials are deposited on a substrate, thermal spray of NiCrAlY followed by YSZ on a substrate of Inconel 718 has been analyzed. Figure 3.8 shows the curvature-temperature input data as a function of time. The first deposition session corresponds to 9 layers of NiCrAlY, the second deposition session corresponds to 10 layers of YSZ. A robotic arm was used for the deposition.

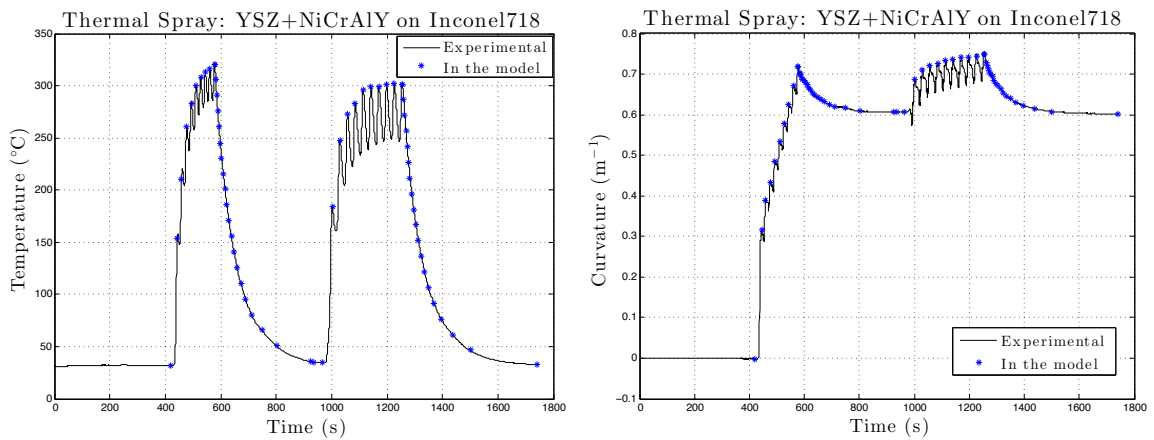


FIGURE 3.8: Points of interest used as input for calculations in multilayer case with two coating materials

Table 3.3 summarizes the parameters used for the residual stress calculation in the computer program.

	Mechanical Properties			Thickness [mm]	Number of Passes
	E [GPa]	α [10^{-6}K^{-1}]	ν		
Substrate	205	13.0	0.30	1.652	—
NiCrAlY Deposit	96.5	12.5	0.30	0.194	9
YSZ Deposit	40	10.0	0.20	0.511	10

TABLE 3.3: Parameters used in deposition of YSZ+NiCrAlY on Inconel 718

Figure 3.9 shows the stress distribution obtained at the end of the coating processing. In addition, Figure 3.10 shows the intrinsic stress developed during the deposition session.

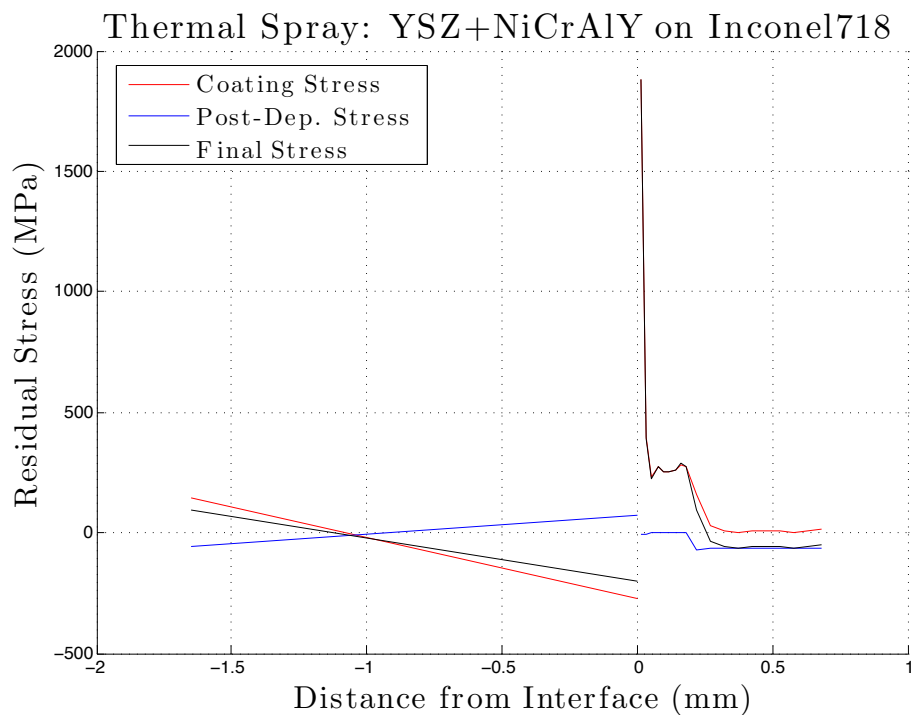


FIGURE 3.9: Final stress distribution in thermal spray YSZ+NiCrAlY on Inconel 718

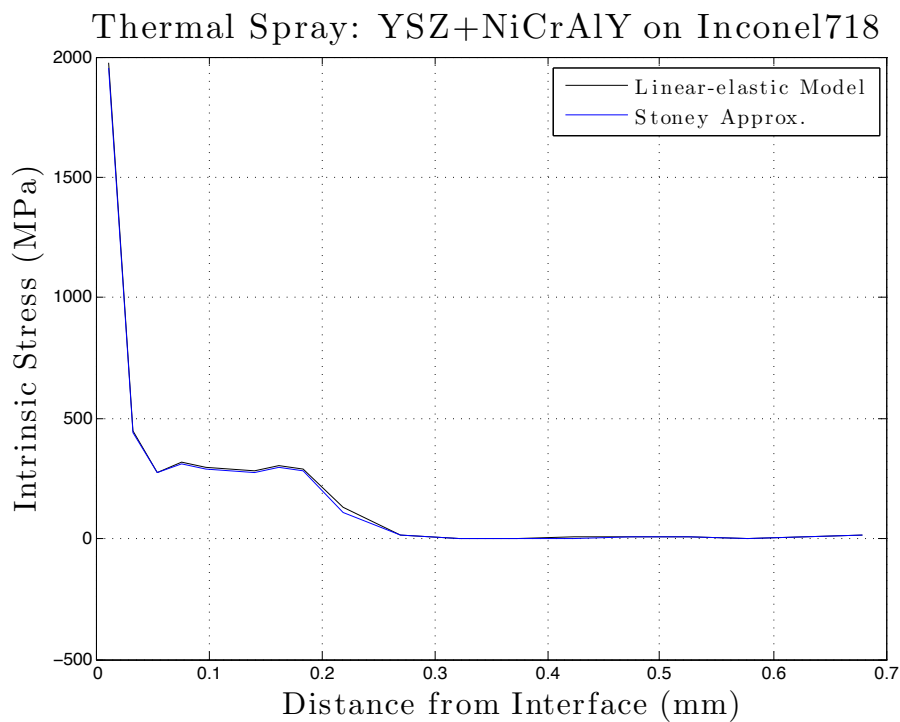


FIGURE 3.10: Comparison between analytic linear elastic model and Stoney formula (YSZ+NiCrAlY)

3.6.3 Multilayer system with one coating material

As an example for a multilayer system where only one coating material has been deposited, thermal spray of YSZ on a substrate of Aluminium has been analyzed. Figure 3.11 shows the curvature-temperature input data as a function of time. The deposition session corresponds to 10 layers of YSZ deposited by a robotic arm.

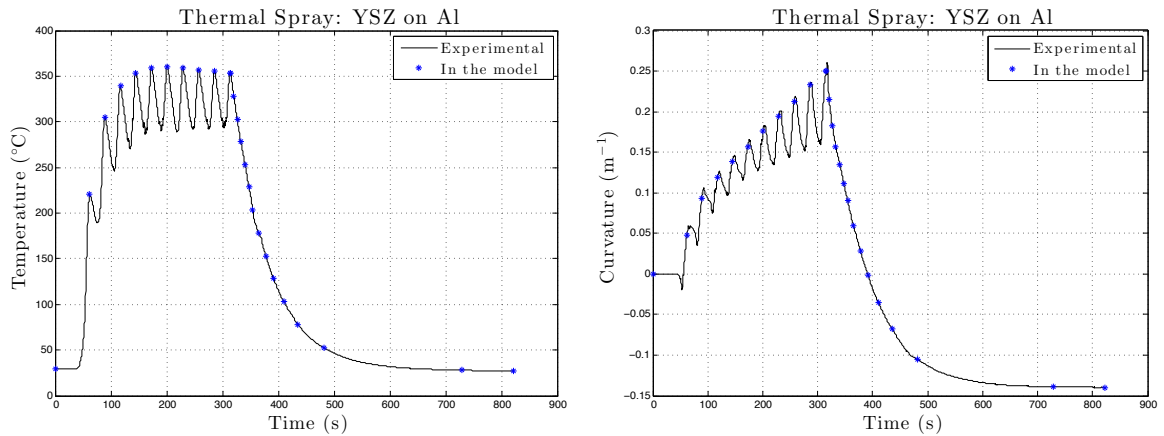


FIGURE 3.11: Points of interest used as input for calculations in multilayer case with one coating material

Table 3.4 summarizes the parameters used for the residual stress calculation in the computer program.

	Mechanical Properties			Thickness [mm]	Number of Passes
	E [GPa]	α [10^{-6}K^{-1}]	ν		
Substrate	70	23.0	0.33	2.25	—
Deposit	40	10.0	0.20	0.644	10

TABLE 3.4: Parameters used in deposition of YSZ on Aluminium

Figure 3.12 shows the stress distribution obtained at the end of the coating processing. In addition, Figure 3.13 shows the intrinsic stress developed at different positions in the deposition stage.

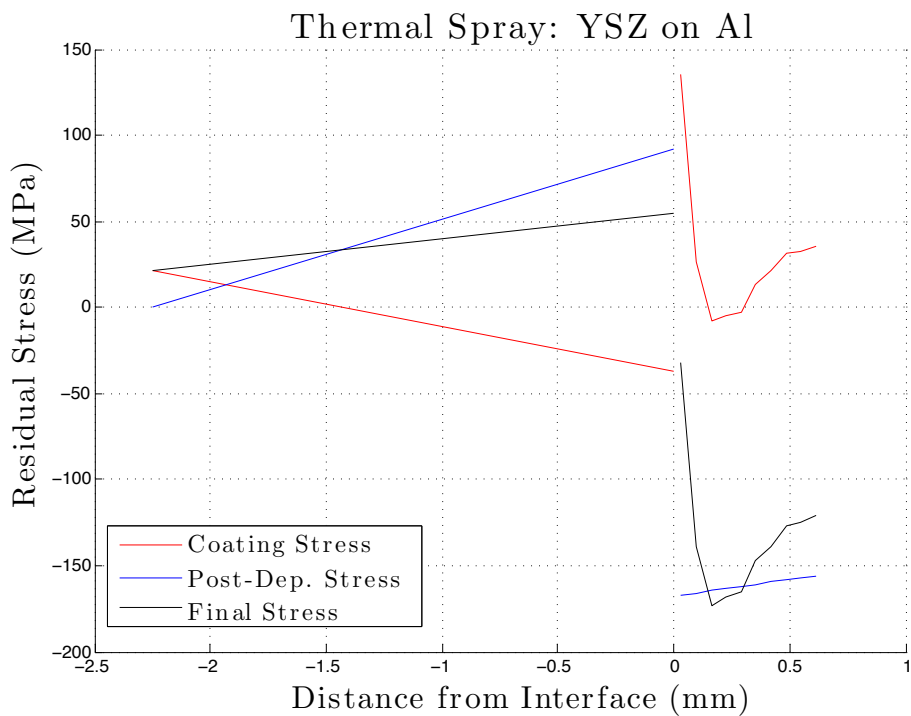


FIGURE 3.12: Final stress distribution in thermal spray YSZ on Aluminium

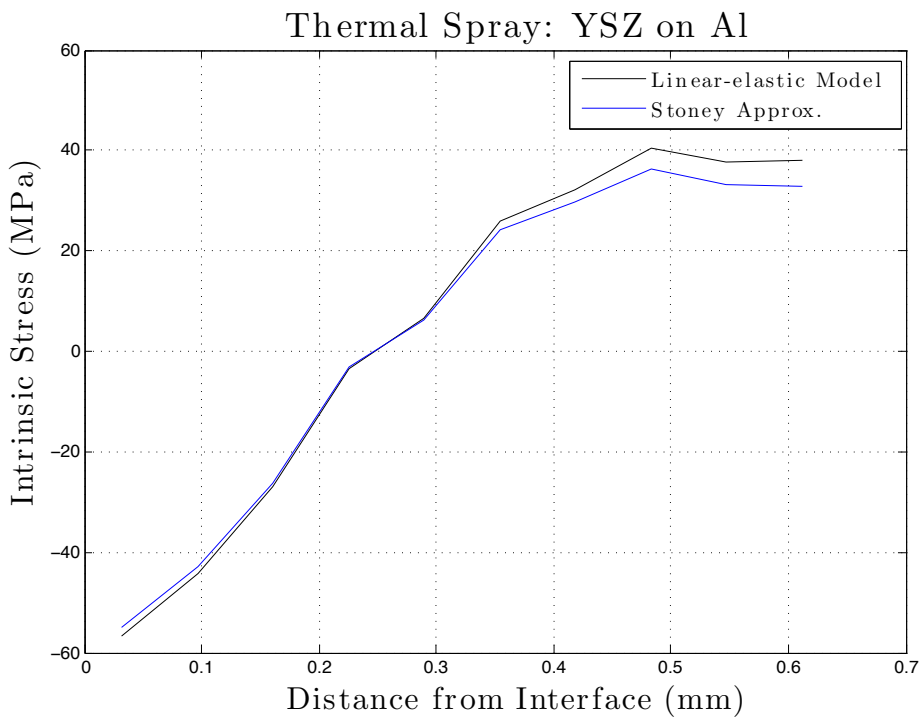


FIGURE 3.13: Comparison between analytic linear elastic model and Stoney formula (YSZ)

3.7 Architecture

Since this program has been implemented in MATLAB[®], every routine has been defined as a function. The Main program is typical *.m file calling the other “main” functions which also call another more basic functions. This architecture has been chosen due to the efficiency granted by MATLAB[®] to work with functions. If another language shall be desired (Python or C# for example) it is recommended to conceive the main routines as *classes* instead of functions. Figure 3.14 shows how all the sequence of functions *.m are related and how the main routines call the subroutines. Appendices I, J, and K contains the subroutines needed for calculating the stress distribution at every point of the process (thermal stress during deposition, evolving stress, and thermal stress during cooling).

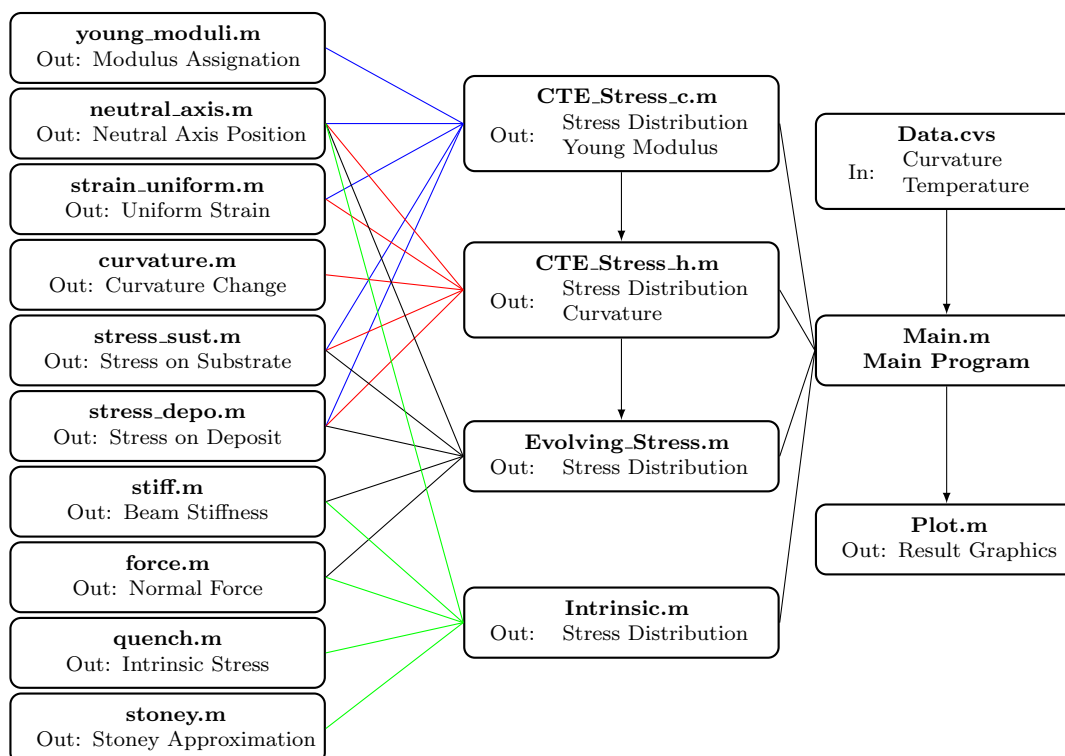


FIGURE 3.14: Program Diagram

Chapter 4

Calculation of Properties for Coating Materials by the Curvature Method

Consider two samples in which the same coating material has been deposited on two different substrates. After the coating process, both composite beams are subjected to heating/cooling *ex-situ* cycles while temperature-curvature data is acquired. Let $E_{(s,1)}, \alpha_{(s,1)}, \nu_{(s,1)}$ be the mechanical properties for the first substrate, $E_{(s,2)}, \alpha_{(s,2)}, \nu_{(s,2)}$ be the mechanical properties for the second substrate, and E_d, α_d be the mechanical properties for the coating material. E_{eff} is the effective elastic modulus for the substrate and it is calculated as follows:

$$E_{eff} = \frac{E_s}{1 - \nu_s}$$

For now on, $E_{(s,1)}, E_{(s,2)}$, and E_d are all effective modulus of each material. From Section 2.4, the curvature change in a cooling/heating cycle post-spraying for the thermal cycle of

the first composite beam can be calculated as:

$$\Delta\kappa_1 = \frac{6E_{(s,1)}t_{(s,1)}E_d h_{(n,1)}(t_{(s,1)} + h_{(n,1)})(\alpha_{(s,1)} - \alpha_d)\Delta T_1}{E_{(s,1)}^2 t_{(s,1)}^4 + 4E_{(s,1)}t_{(s,1)}^3 E_d h_{(n,1)} + 6E_{(s,1)}t_{(s,1)}^2 E_d h_{(n,1)}^2 + 4E_{(s,1)}t_{(s,1)} E_d h_{(n,1)}^3 + E_d^2 h_{(n,1)}^4}$$

and for the second composite beam:

$$\Delta\kappa_2 = \frac{6E_{(s,2)}t_{(s,2)}E_d h_{(n,2)}(t_{(s,2)} + h_{(n,2)})(\alpha_{(s,2)} - \alpha_d)\Delta T_2}{E_{(s,2)}^2 t_{(s,2)}^4 + 4E_{(s,2)}t_{(s,2)}^3 E_d h_{(n,2)} + 6E_{(s,2)}t_{(s,2)}^2 E_d h_{(n,2)}^2 + 4E_{(s,2)}t_{(s,2)} E_d h_{(n,2)}^3 + E_d^2 h_{(n,2)}^4}$$

In equations above $t_{(s,i)}$ is the substrate deposit for beam i and $h_{(n,i)} = nt_{(d,i)}$ is the coating thickness for beam i . Let:

$$\begin{aligned} A_i &= 6E_{(s,i)}t_{(s,i)}h_{(n,i)}(t_{(s,i)} + h_{(n,i)}) \\ B_i &= h_{(n,i)}^4 \\ C_i &= 4E_{(s,i)}t_{(s,i)}^3 h_{(n,i)} + 6E_{(s,i)}t_{(s,i)}^2 h_{(n,i)}^2 + 4E_{(s,i)}t_{(s,i)} h_{(n,i)}^3 \\ D_i &= E_{(s,i)}^2 t_{(s,i)}^4 \\ F_i &= \frac{\Delta\kappa_i}{A_i \Delta T_i} \end{aligned}$$

for $i \in \{1, 2\}$. Thus, the following system of equations which variables are E_d and α_d can be constructed:

$$\begin{cases} F_1 &= \frac{E_d \alpha_{(s,1)} - E_d \alpha_d}{B_1 E_d^2 + C_1 E_d + D_1} \\ F_2 &= \frac{E_d \alpha_{(s,2)} - E_d \alpha_d}{B_2 E_d^2 + C_2 E_d + D_2} \end{cases}$$

Now, let $X_i = F_i B_i$, $Y_i = F_i C_i - \alpha_{(s,i)}$, and $Z_i = F_i D_i$. Then the system of equations can be written as:

$$\begin{cases} X_1 E_d^2 + Y_1 E_d + Z_1 &= -E_d \alpha_d \\ X_2 E_d^2 + Y_2 E_d + Z_2 &= -E_d \alpha_d \end{cases}$$

Subtracting both equation the following quadratic equation is obtained:

$$aE_d^2 + bE_d + c = 0$$

where $a = X_1 - X_2$, $b = Y_1 - Y_2$, $c = Z_1 - Z_2$. Usually, the effective elastic modulus has a magnitude of 10^{11} Pascals, i.e $E_{(s,i)} \sim \mathcal{O}(10^{11})$; in the other hand, the thickness are usually given in millimeters, i.e $t_{(s,i)}, h_{(n,i)} \sim \mathcal{O}(10^{-3})$, and the coefficient of thermal expansion is given in micro units, i.e $\alpha_{(s,1)} \sim \mathcal{O}(10^{-6})$. The change of curvature is usually less than 1 m^{-1} and the temperature in the thermal cycle is around $200 \text{ }^\circ\text{C}$. Then $\Delta\kappa_i \sim \mathcal{O}(10^{-1})$, and $\Delta T_1 \sim \mathcal{O}(10^2)$.

It is easy to show that $A_i \sim \mathcal{O}(10^2)$, then $F_i \sim \mathcal{O}(10^{-5})$. Similarly, $B_i \sim \mathcal{O}(10^{-12})$, $C_i \sim \mathcal{O}(10^{-1})$, and $D_i \sim \mathcal{O}(10^{10})$. Finally, $a \sim \mathcal{O}(10^{-17})$, $b \sim \mathcal{O}(10^{-6})$, and $c \sim \mathcal{O}(10^5)$.

Note that $a \ll c$. To avoid *catastrophic cancellation* while solving the quadratic equation in a computer software, it is recommendable to use the linear approximation ($a \approx 0$); otherwise, the quadratic formula will solve it. In conclusion, to calculate the mechanical properties of the coating material it suffices to solve the following equations¹:

$$E_d = \frac{-b - \sqrt{b^2 - 4ac}}{2a}$$

$$\alpha_d = -\frac{X_1 E_d^2 + Y_1 E_d + Z_1}{E_d}$$

It is noteworthy that if only one sample is available for the thermal cycle test, either the modulus or the CTE must be known or assumed. The elastic modulus in thermal spray coatings is regularly a fraction (0.3 - 0.8) of the bulk material. Therefore, the CTE is most commonly assumed to be of the bulk material.

¹The sign of the discriminant in the quadratic equation has been determined experimentally, the plus sign will give negative answers for the elastic modulus

4.1 Determination of mechanical properties for NiCr

Elastic modulus and coefficient of thermal expansion has been calculated as a function of temperature for a NiCr coating. In order to calculate such properties two different materials has been used as substrates for NiCr, aluminum Al6061 and stainless steel SS316. Each composite beam has been taken to two consecutive heating/cooling thermal cycles as shown in Figure 4.1. The linear elastic behavior is clear in the experimental results.

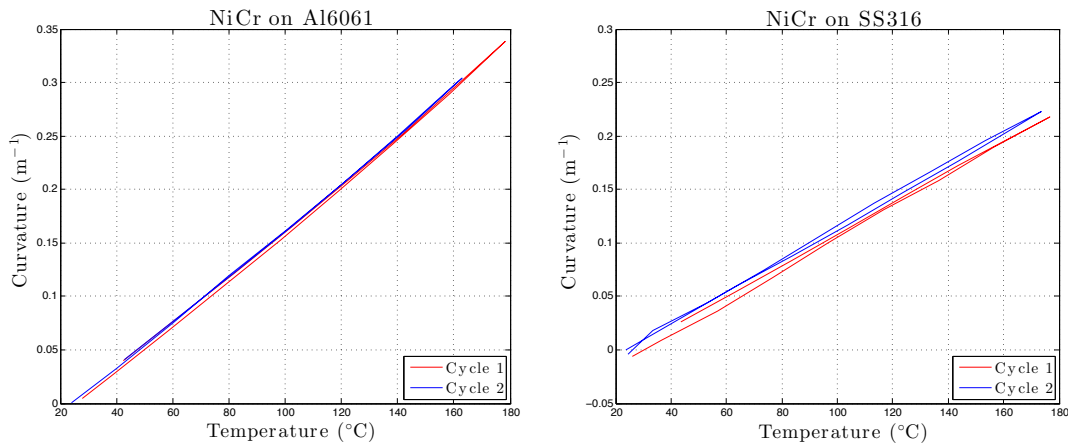


FIGURE 4.1: Thermal cycles for NiCr on both, Al6061 and SS316

Parameters used in equations described previously are summarized in Table 4.1. In order to improve the precision of the answer, the coefficient of thermal expansion has been considered as temperature dependent.

Property	Material		
	NiCr	Al6061	SS316
Elastic Modulus [GPa]	—	68.9	193
Poisson Ratio	—	0.33	0.33
CTE [10^{-6}K^{-1}]	—	$22.76 + 0.0185T$	$16.5 + 0.0071T$
Thickness (1 st beam) [mm]	0.2330*	3.1455	—
Thickness (2 nd beam) [mm]	0.2316*	—	1.4902

TABLE 4.1: Parameters used for thermal cycle calculations

* Samples were sprayed simultaneously. Processing manner is similar to the processing described in [14]

The system of equations for E_d and α_d is solved for different temperature intervals. The temperature range of the experiment (between 20 and 180 Celsius degrees) is divided in smaller segments in order to have several point to interpolate a linear equation describing the dependence in temperature of the properties. If the partition is finer then the results can be noisy, but if the partition is too rough then accuracy can be lost. In this case the selected intervals are of 20°C each one in both cycles. Results can be observed in Figure 4.2 and the resultant dependency can be stated as:

$$E_d = 195.9 + 0.1647T \text{ [GPa]}$$

$$\alpha_d = 12 + 9.335 \times 10^{-3}T \text{ [}10^{-6}\text{C}^{-1}\text{]}$$

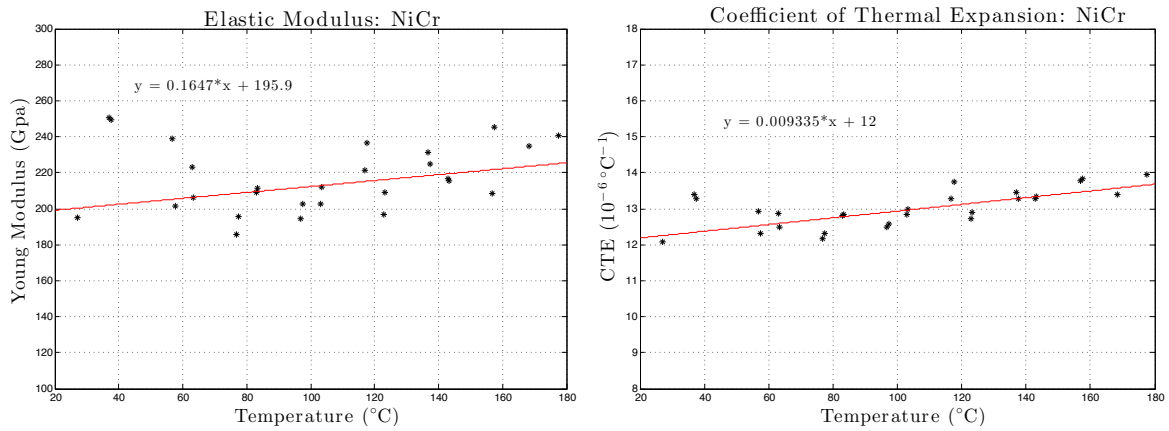


FIGURE 4.2: Elastic modulus and CTE as a function of temperature

Remark 4.1. Note that this elastic modulus is in fact the effective elastic modulus for an in-plane geometry.

Chapter 5

Sensitivity Analysis

Consider a heating/cooling *ex-situ* experiment as in Chapter 4. In this section, the sensitivity of the measurements of curvature-temperature with respect to the material properties of the substrate and the deposit is analyzed. First, recall the curvature equation deduced in Section 2.4:

$$\Delta\kappa = \frac{6E_s t_s E_d h_n (t_s + h_n) (\alpha_s - \alpha_d) \Delta T}{E_s^2 t_s^4 + 4E_s t_s^3 E_d h_n + 6E_s t_s^2 E_d h_n^2 + 4E_s t_s E_d h_n^3 + E_d^2 h_n^4}$$

where h_n is the total coating thickness at the end of the deposition process. Any infinitesimal measurement along the thermal cycle curve denotes a curvature change $d\kappa$ as a response to a temperature gradients dT . This *ex-situ* experiment is linear elastic, and therefore the curve κ vs T is a straight line as in Figure 4.1. This misfit strain due to temperature difference between substrate and deposit is $\Delta\varepsilon = (\alpha_s - \alpha_d)\Delta T$. The slope of the experimental curve $M = d\kappa/d\varepsilon$ is constant along the process.

In this section, the sensitivity of the thermal cycling κ vs T test is studied in order to:

1. Maximize the magnitude of the beam deflection in the test to aver the resolution of the technique.

2. Deduce the error of the model when high sensitivity is expected with respect to the ratio of the thickness (t_s/h_n) or the ratio of the elastic moduli between coating and substrate (E_s/E_d).

Thus, the slope M can be calculated as:

$$\begin{aligned}
 M &= \frac{6E_s t_s E_d h_n (t_s + h_n)}{E_s^2 t_s^4 + 4E_s t_s^3 E_d h_n + 6E_s t_s^2 E_d h_n^2 + 4E_s t_s E_d h_n^3 + E_d^2 h_n^4} \\
 &= \frac{6t_s h_n (t_s + h_n)}{\frac{E_s}{E_d} t_s^4 + 4t_s^3 h_n + 6t_s^2 h_n^2 + 4t_s h_n^3 + \frac{E_d}{E_s} h_n^4} \\
 &= \frac{6 \left(\frac{1}{h_n} + \frac{1}{t_s} \right)}{\frac{E_s}{E_d} \frac{t_s^2}{h_n^2} + 4 \frac{t_s}{h_n} + 6 + 4 \frac{h_n}{t_s} + \frac{E_d}{E_s} \frac{h_n^2}{t_s^2}} \\
 &= \frac{1}{t_s} \frac{6 \left(\frac{t_s}{h_n} + 1 \right)}{\frac{E_s}{E_d} \frac{t_s^2}{h_n^2} + 4 \frac{t_s}{h_n} + 6 + 4 \frac{h_n}{t_s} + \frac{E_d}{E_s} \frac{h_n^2}{t_s^2}}
 \end{aligned}$$

Let's define:

$$x = \frac{t_s}{h_n} \quad \text{and} \quad y = \frac{E_s}{E_d}$$

Then the slope turns out to be:

$$M = \frac{1}{t_s} \frac{6(x+1)}{yx^2 + 4x + 6 + 4\frac{1}{x} + \frac{1}{yx^2}} = \frac{1}{t_s} f(x, y)$$

In this analysis, a substrate thickness must be given ($t_s = \text{constant}$). Since the slope is a function of x and y , i.e $M = 1/t_s f(x, y)$, it is necessary to establish how M varies when x and y vary. In most of the cases $t_s > h_n$ and $E_s > E_d$; thus, the analysis focuses on studying the variation when $x \in [0.5, 30]$ and $y \in [0.5, 10]$ (typical experimental values).

Figure 5.1 shows the function $f(x, y)$ for the values considered for x and y . Note that when x and y tend to the maximum values ($x \rightarrow 30$ and $y \rightarrow 10$), the value of the function tends to

zero. This means that when the thickness of the coating is much thinner than the substrate, and the substrate is significantly stiffer than the coating the effect of bending is negligible.

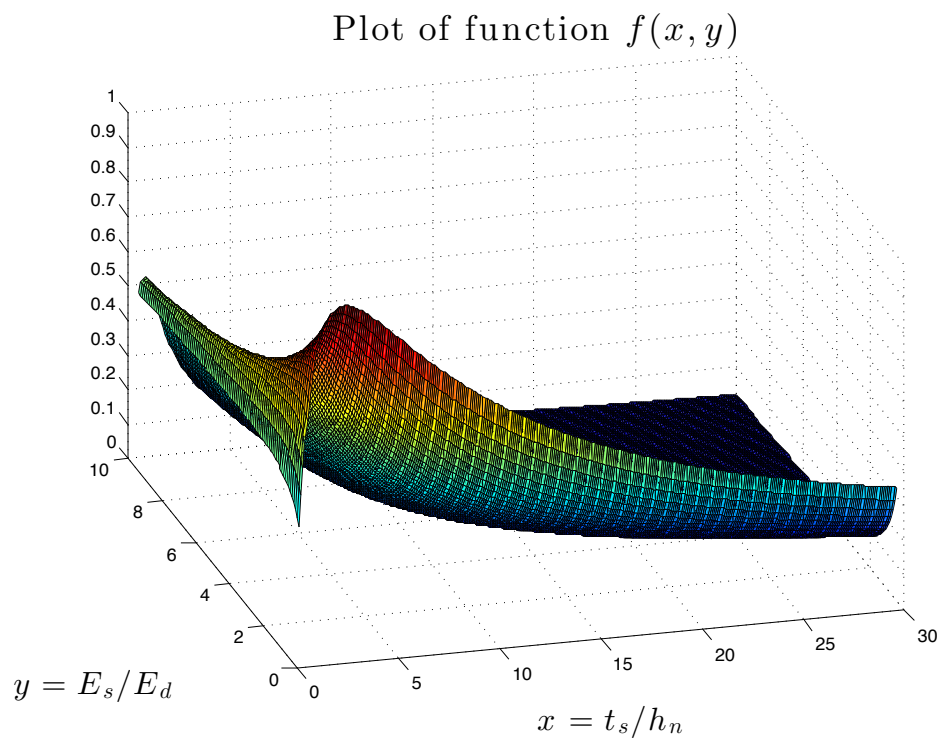


FIGURE 5.1: 3D plot for the function $f(x, y)$ for $x \in [0.5, 30]$ and $y \in [0.5, 10]$

Figure 5.2 shows a contour plot of the function $f(x, y)$. Note that the maximum value of the function is reached at the point $(x, y) = (2.7, 0.5)$ which is $f_{max} \approx 1$.

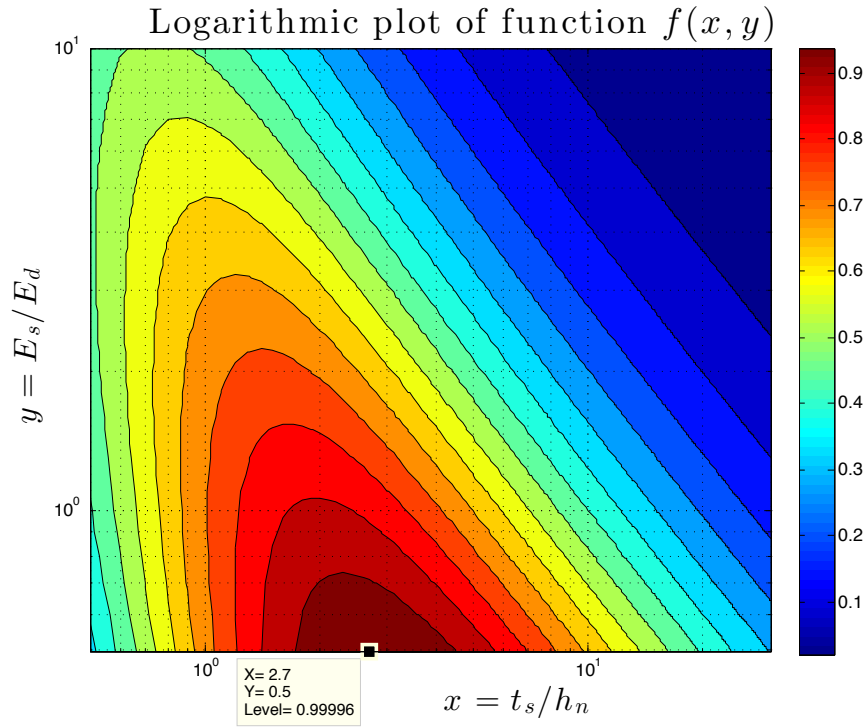


FIGURE 5.2: Contour plot for the function $f(x, y)$ for $x \in [0.5, 30]$ and $y \in [0.5, 10]$

To determine the sensitivity of and how M varies when x varies it is necessary to calculate the following partial derivative:

$$\begin{aligned}
 \frac{\partial M}{\partial x} &= \frac{1}{t_s} \frac{6 \left(yx^2 + 4x + 6 + 4\frac{1}{x} + \frac{1}{yx^2} \right) - 6(x+1) \left(2yx + 4 - 4\frac{1}{x^2} - 2\frac{1}{yx^3} \right)}{\left(yx^2 + 4x + 6 + 4\frac{1}{x} + \frac{1}{yx^2} \right)^2} \\
 &= \frac{6 yx^2 + 4x + 6 + 4\frac{1}{x} + \frac{1}{yx^2} - 2yx^2 - 4x + 4\frac{1}{x} + 2\frac{1}{yx^2} - 2yx - 4 + 4\frac{1}{x^2} + 2\frac{1}{yx^3}}{t_s \left(yx^2 + 4x + 6 + 4\frac{1}{x} + \frac{1}{yx^2} \right)^2} \\
 &= \frac{1}{t_s} \frac{6 \left(-yx^2 + 8\frac{1}{x} + 3\frac{1}{yx^2} - 2yx + 4\frac{1}{x^2} + 2\frac{1}{yx^3} + 2 \right)}{\left(yx^2 + 4x + 6 + 4\frac{1}{x} + \frac{1}{yx^2} \right)^2} \\
 \frac{\partial M}{\partial x} &= \frac{1}{t_s} M_x(x, y)
 \end{aligned}$$

Similarly, to calculate how M varies if y varies it suffices to compute:

$$\frac{\partial M}{\partial y} = \frac{1}{t_s} \frac{-6(x+1) \left(x^2 - \frac{1}{y^2 x^2} \right)}{\left(yx^2 + 4x + 6 + 4\frac{1}{x} + \frac{1}{yx^2} \right)^2}$$

$$\frac{\partial M}{\partial y} = \frac{1}{t_s} M_y(x, y)$$

Figure 5.3 shows the function $M_x(x, y)$ for the values considered for x and y . Note that for $x \geq 5$ the value for M_x is almost constant (and equal to zero). Similarly, Figure 5.4 shows the plot for function $M_y(x, y)$; in this case, for $y \geq 5$ the value for M_y is almost constant (and equal to zero).

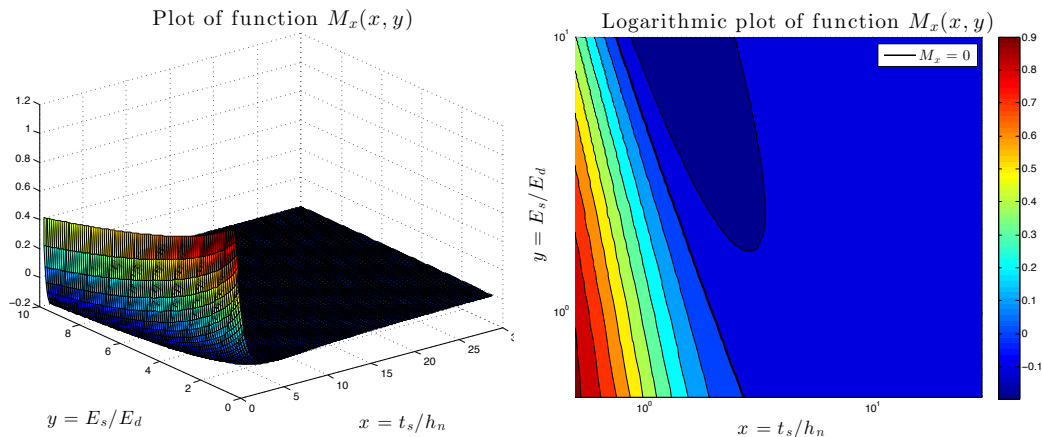


FIGURE 5.3: Plot for the function $M_x(x, y)$ for $x \in [0.5, 30]$ and $y \in [0.5, 10]$

Recall that $d\varepsilon = (\alpha_s - \alpha_d)dT$, and $\alpha \sim \mathcal{O}(10^{-6})$, $T \sim \mathcal{O}(10^2)$; thus, $d\varepsilon \sim \mathcal{O}(10^{-4})$. In the other hand, $d\kappa \sim \mathcal{O}(10^{-1})$, and $t_s \sim \mathcal{O}(10^{-3})$. Since $f(x, y) = t_s \frac{d\kappa}{d\varepsilon}$ then $f(x, y) \sim \mathcal{O}(1)$.

Lets consider an error less than 5% as negligible; in other words, if $M_x, M_y < 0.05$ then the error is considered as negligible while measuring M . Previously, it was concluded that for $x \geq 5$ and $y \geq 5$, both functions (M_x and M_y) reach a constant value; which is actually less

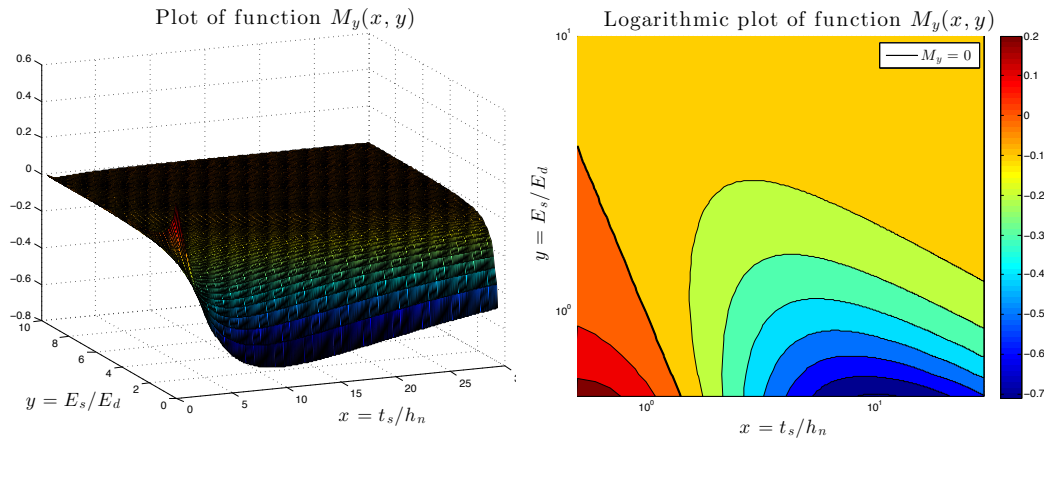


FIGURE 5.4: Plot for the function $M_y(x, y)$ for $x \in [0.5, 30]$ and $y \in [0.5, 10]$

that the 5% relative error as it can be appreciated in Figure 5.5. Therefore, if $x \geq 5$ and $y \geq 5$ then $M_x = M_y \approx 0$.

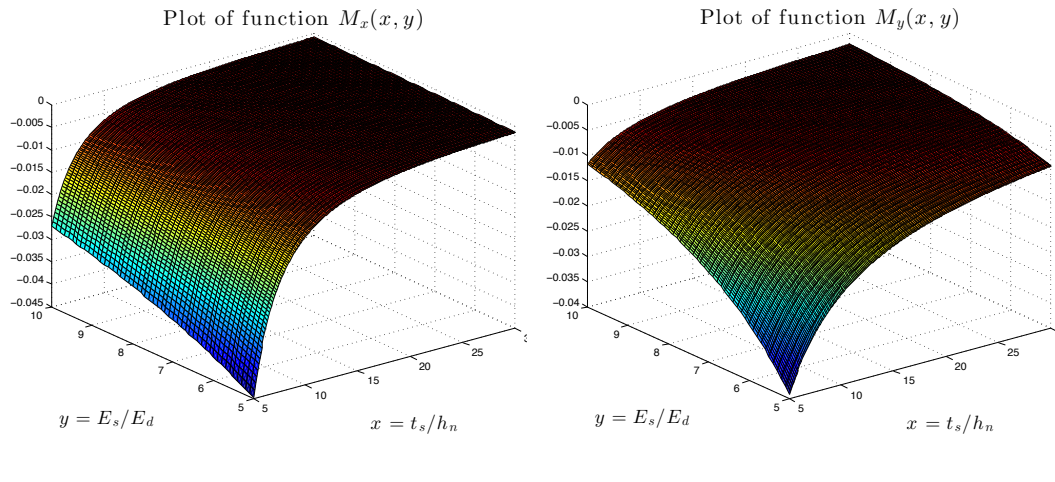


FIGURE 5.5: Negligible region for $M_x(x, y)$ and $M_y(x, y)$

Consider the region where $x \in [0.5, 5]$ and $y \in [5, 10]$. In order to reduce at the minimum the functions M_x and M_y , the point (x, y) must be chosen such that it lies around zero in both plots, $M_x(x, y)$ and $M_y(x, y)$. Recall from Figure 5.4 that in this region almost every value of $M_y(x, y)$ is constant, thus it suffices to stay near zero for $M_x(x, y)$. Figure 5.6 shows a band where $M_x(x, y) = 0 \pm 0.05$, in which any value is acceptable for minimizing the error.

In conclusion, if $x \in [0.5, 5]$ and $y \in [5, 10]$, a point (x, y) should be picked in such a way that it lies within the band described previously in Figure 5.6, note that the x axis was drawn in logarithmic scale.

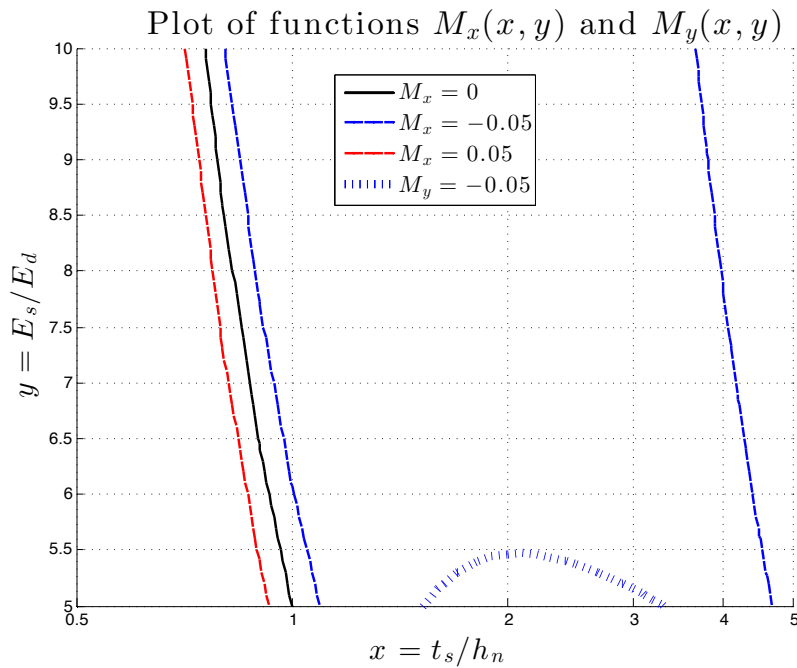


FIGURE 5.6: Values for $M_x(x, y)$ and $M_y(x, y)$ for $x \in [0.5, 5]$ and $y \in [5, 10]$

Consider the region where $x \in [5, 30]$ and $y \in [0.5, 5]$. Same as before, the point (x, y) needs to be chosen in such a way that it lies around zero in both plots, $M_x(x, y)$ and $M_y(x, y)$. Recall from Figure 5.3 that in this region almost every value of $M_x(x, y)$ is constant, thus it suffices to stay around zero for $M_y(x, y)$. Note in Figure 5.7 that there is no line where $M_y = 0$, but there is one where $M_y = -0.05$. In Figure 5.4 it is possible to see that for values above the line $M_y = -0.05$ the values are nearly constant. Thus, trying to minimize the relative error in the region where $x \in [5, 30]$ and $y \in [0.5, 5]$, it is necessary to pick a point above the line $M_y = -0.05$. Note that the x axis was drawn in logarithmic scale.

Let $x \in [0.5, 5]$ and $y \in [0.5, 5]$. Figure 5.8 shows the values of the function $f(x, y)$ in this

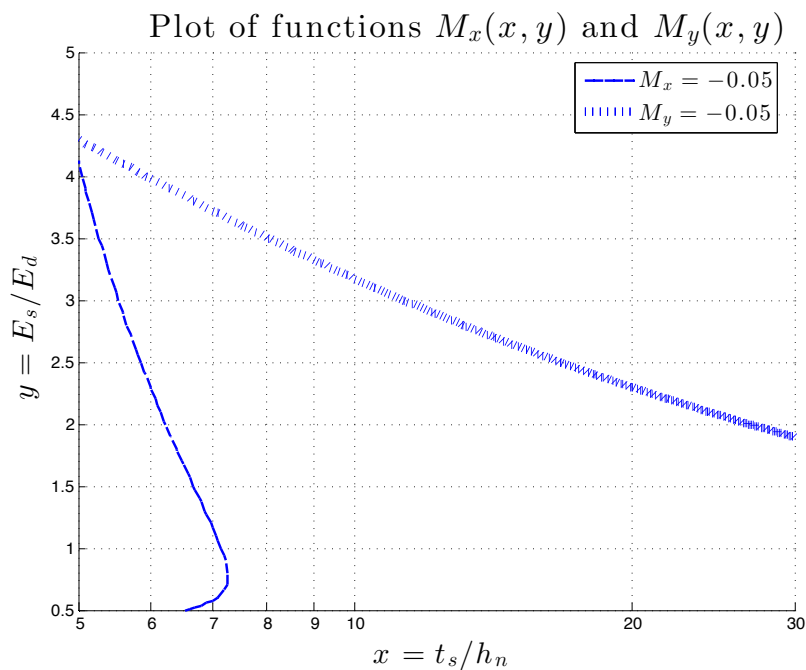


FIGURE 5.7: Values for $M_x(x, y)$ and $M_y(x, y)$ for $x \in [5, 30]$ and $y \in [0.5, 5]$

region, Figure 5.9 shows the values of the function $M_x(x, y)$, and Figure 5.10 shows the values of the function $M_y(x, y)$.

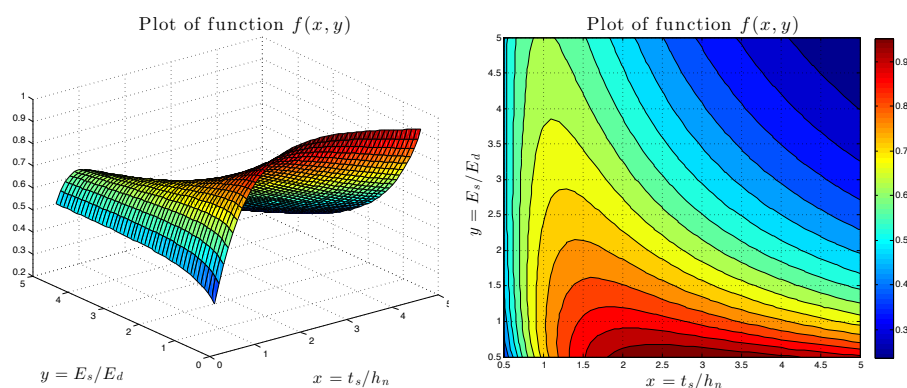


FIGURE 5.8: Plot of function $f(x, y)$ for $x \in [0.5, 5]$ and $y \in [0.5, 5]$

To select optimum values of (x, y) and minimize the error $(M_x(x, y), M_y(x, y))$ in the heating cycle test, the point (x, y) must be chosen where $M_x = 0$ and $M_y = 0$. Figure 5.11 shows

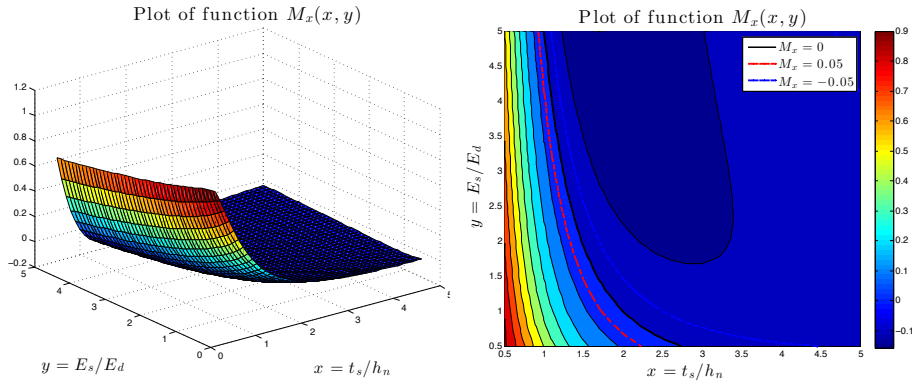


FIGURE 5.9: Plot of function $M_x(x, y)$ for $x \in [0.5, 5]$ and $y \in [0.5, 5]$

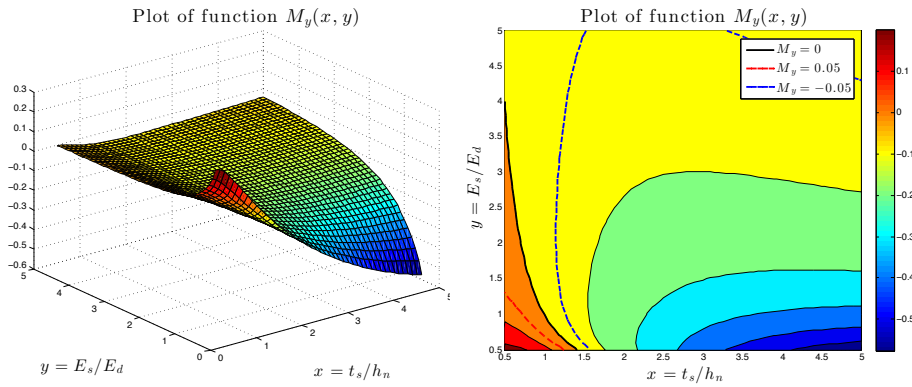


FIGURE 5.10: Plot of function $M_y(x, y)$ for $x \in [0.5, 5]$ and $y \in [0.5, 5]$

asymptotic lines for $M_x = 0$ and for $M_y = 0$. Note that there is not a point of intersection where $M_x = M_y = 0$, so it is needed to find a point that lies within the regions $A = \{(x, y) \mid M_x(x, y) = 0 \pm 0.05\}$ and $B = \{(x, y) \mid M_y(x, y) = 0 \pm 0.05\}$. Finally, to minimize the relative error in the region where $x, y \in [0.5, 5]$ it is necessary to pick a point $(x, y) \in A \cap B$. Figure 5.11 shows the region where such point should be chosen, note that the x axis was drawn in logarithmic scale.

In conclusion, given a substrate and a coating material, it is possible to determine the coating thickness to minimize the error while measuring κ and T in an ex-situ experiment. Defining $x = t_s/h_n$ and $y = E_s/E_d$, typically the following values: $x \in [0.5, 30]$ and $y \in [0.5, 10]$ are

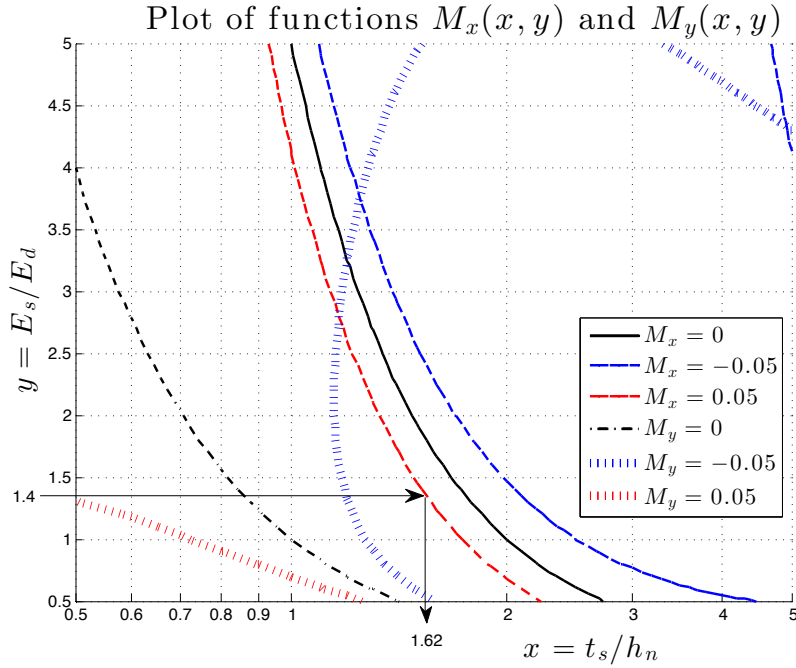


FIGURE 5.11: Values for $M_x(x, y)$ and $M_y(x, y)$ for $x, y \in [0.5, 5]$

expected. Table 5.1 presents a quick way to use Figures 5.6, 5.7 and 5.11 presented in this section. Finally, pick x such that minimizes the value for M_x and M_y simultaneously.

Region		Action
Value of y	Desirable value of x	
$y \in [5, 10]$	$x \in [5, 30]$	Pick any point (x, y) , $M_x = M_y \approx 0$
	$x \in [0.5, 5]$	Pick a point near the line $M_x = 0$ in Figure 5.6
$y \in [0.5, 5]$	$x \in [5, 30]$	Pick a point above the line $M_y = -0.05$ in Figure 5.7
	$x \in [0.5, 5]$	Pick a point where M_x and M_y are minimal in Figure 5.11

TABLE 5.1: Actions to take given the value of $y = E_s/E_d$

Example 5.1. Suppose that we have a metal sheet of stainless steel SS316 ($E_s = 193\text{GPa}$) with thickness of 3mm. We want to coat this substrate with NiCr ($E_d = 140\text{GPa}$) and we would like to know how much deposit we should use in order to obtain accurate measurements during a given coating process. First of all, we get the value for the effective modulus ratio, i.e $y = 1.38$ (supposing that both materials have the same Poisson ratio). Check Figure 5.11.

Note that there is not any point with $y = 1.38$ such that $(x, y) \in A \cap B$ where $A = \{(x, y) \mid M_x(x, y) = 0 \pm 0.05\}$ and $B = \{(x, y) \mid M_y(x, y) = 0 \pm 0.05\}$, then we are forced to favor the region where M_x is minimum (since this region is the narrowest) so we choose the point on the line $M_x = 0.05$. This point is around $10^{0.21} \approx 1.62$ (recall that $2 \approx 10^{0.3}$). Finally, since $t_s = 3$ and $x = t_s/h_n$ we conclude that the coating thickness should be $h_n = 1.85\text{mm}$.

Remark 5.1. Since the analysis takes differential intervals $d\kappa$ and dT , it is possible to apply the same conclusions to the in-situ experiment described in Chapter 2 where the curve κ vs T is not a straight line.

Chapter 6

Conclusion

Tsui-Clyne analytical model for intrinsic stress and Hsueh analytical model for thermal stress have been used as a starting point for the project. Intrinsic and thermal stress have been added together in the same analysis for a more real model of stress distribution. Results allow to track the stress distribution in the composite beam at any stage of the entire coating process (including deposition stage and cooling stage). A multilayer linear elastic computer model for different coating materials in the same process has been implemented in MATLAB[®]. Moreover, a multilayer linear elastic analysis for coating at both sides of the substrate has been developed.

The results obtained indicate that there is a relatively high contribution of residual stress in the deposition of the first layer in each deposition session. Although this effect is due to both, intrinsic and thermal stress, intrinsic stress is predominant. The residual stress plots indicates that in between different materials there is a tensile force acting.

Temperature-Curvature data in an ex-situ experiment is enough to determine the mechanical properties for the coating material as a function of temperature. A linear interpolation is enough to guarantee an accurate value of mechanical properties in a given interval. Data

filtering is necessary in order to reduce the sensitivity of the slope $d\kappa/dT$. Sensitivity analysis allows to determine the appropriate relation between substrate and deposit in order to get an accurate measurements of curvature-temperature regardless the sensor accuracy.

The curvature method allows to experimentally calculate the intrinsic stress distribution for a given deposition process of a certain number of layers for different coating materials onto a given substrate. This stress can be applied to calculate the residual stress distribution for coating process where curvature measures can be neglected (bulky substrate. This type of processing is really common in the coating industry.

Finally, the curvature method gives a way to select the coating thickness required to minimize the relative errors while taking curvature-temperature measurements in *ex-situ* and *in-situ* experiments.

Appendix A

Proof of Summation Identities

$$\begin{aligned}\sum_{j=1}^n (2j - 1) &= 2 \sum_{j=1}^n j - \sum_{j=1}^n 1 \\ &= n(n + 1) - n \\ &= n^2 + n - n\end{aligned}$$

$$\sum_{j=1}^n (2j - 1) = n^2$$

$$\begin{aligned}\sum_{j=1}^n (3j^2 - 3j + 1) &= 3 \sum_{j=1}^n j^2 - 3 \sum_{j=1}^n j + \sum_{j=1}^n 1 \\ &= n^3 + 3n^2/2 + n/2 - 3n^2/2 - 3n/2 + n \\ &= n^3\end{aligned}$$

Appendix B

Program Main Routine

```
1  %%%%%%%%%%%%%%%%%%%%%%%%%%%%%%%%%%%%%%%%%%%%%%%%%%%%%%%%%%%%%%%%%%%%%%%%%%
2  % Analytic Linear-Elastic Analysis of Stress Distribution in %
3  % Thermal Spray Coatings %
4  % Multilayer System %
5  % Bryan Maldonado %
6  % Version 2.0 %
7  %%%%%%%%%%%%%%%%%%%%%%%%%%%%%%%%%%%%%%%%%%%%%%%%%%%%%%%%%%%%%%%%%%%%%%%%%%
8
9  %% Program Initialization
10
11 clear all
12 close all
13
14 Process = Thermal Spray: NiCr on AISI 1018 ;
15 filename = NiCr.on.AISI1018.csv ;
16
17 %% Substrate Data
18
19 E_s = 200e9; % Elastic Modulus [Pa]
20 a_s = 12.2e-6; % CTE [C^-1]
21 nu_s = 0.29; % Poisson Ratio
22 t_s = 2.431e-3; % Substrate Thickness [m]
23
24 %% Deposits Data
25
26 E_d1 = 140e9; % Elastic Modulus [Pa]
27 a_d1 = 14e-6; % CTE [C^-1]
28 nu_d1 = 0.3; % Poisson Ratio
29 N_1 = 20; % Number of passes
30 w_1 = 0.893e-3; % Substrate Thickness [m]
31
32 %% Deposit Properties summary
33
34 E_d1 = E_d1/(1-nu_d1);
35
36 E_d = [E_d1 E_d1];
37 a_d = [a_d1 a_d1];
38 N = [N_1/2 N_1/2];
39 w = [w_1/2 w_1/2];
```

```
40
41 %% Process Data
42
43 [~,~,~,~, Temp_h, Kappa_h, ~, Temp_c, Kappa_c] = ReadData2(filename);
44
45 %% Thermal Stress in Cooling Stage
46
47 [sigma_s_c, sigma_d_c, E_d] = CTEStress_c(N, w, a_d, E_d, t_s, a_s, ...
48                                     E_s, nu_s, Kappa_c, Temp_c);
49
50 %% Thermal Stress in Coating Stage
51
52 [sigma_s_h, sigma_d_h, dkappa_h] = CTEStress_h(N, w, a_d, E_d, t_s, ...
53                                     a_s, E_s, nu_s, Temp_h);
54
55 %% Evolving Stress in Coating Stage
56
57 [sigma_s, sigma_d] = EvolvingStress(N, w, E_d, t_s, E_s, nu_s, ...
58                                     Kappa_h, dkappa_h);
59
60 %% Intrinsic Stress
61
62 [sigma_q, sigma_st] = Intrinsic(N, w, E_d, t_s, E_s, nu_s, Kappa_h, dkappa_h);
63
64 %% Results
65
66 Plot_Result(N, w, t_s, sigma_s, sigma_d, sigma_s_h, sigma_d_h, sigma_s_c, ...
67             sigma_d_c, sigma_q, sigma_st, Process, filename);
```

Appendix C

Data Acquisition

```
1 % Input Data
2 % Data acquired from external program
3
4 function [Time, Temp, Kappa, Time_h, Temp_h, Kappa_h, Time_c, Temp_c, ...
5           Kappa_c] = ReadData2(filename)
6 %% Curvature - Temperature Input
7
8 fileID = fopen(filename);
9 Data = textscan(fileID, repmat( %f ,1,3), Delimiter , , , ...
10                        HeaderLines ,1, EmptyValue ,NaN);
11 fclose(fileID);
12
13 Time = Data{1};
14 Temp = Data{2};
15 Kappa = Data{3};
16
17 %% Signal filtering
18
19 Time( isnan(Time) ) = [];
20 Temp( isnan(Temp) ) = [];
21 Kappa = Kappa( 1:length(Time) );
22
23 delta_t = 0.25;
24 tempol = Time(1):delta_t:Time(end);
25 index = zeros( size(tempol) );
26
27 for i = 1:length(tempol);
28     [~, index(i)] = min( abs( Time - tempol(i) ) );
29 end
30
31 Time = [Time(index) ; Time(end) ];
32 Temp = [Temp(index) ; Temp(end) ];
33 Kappa = [Kappa(index); Kappa(end)];
34
35 %% Points of interes
36
37 [~,ini] = min( abs(Time - 57.1) );
38 [~,r1] = min( abs(Time - 68.3) );
39 [~,r2] = min( abs(Time - 81.1) );
```



```

40 [~,r3] = min( abs(Time - 92.2) );
41 [~,r4] = min( abs(Time - 103.3) );
42 [~,r5] = min( abs(Time - 114.6) );
43 [~,r6] = min( abs(Time - 126.1) );
44 [~,r7] = min( abs(Time - 137.1) );
45 [~,r8] = min( abs(Time - 147.1) );
46 [~,r9] = min( abs(Time - 158.3) );
47 [~,r10] = min( abs(Time - 168.4) );
48 [~, last] = min( abs(Time - 276.8) );
49
50 time_h11 = Time ( [ini r1 r2 r3 r4 r5 r6 r7 r8 r9 r10] );
51 kappa_h11 = Kappa( [ini r1 r2 r3 r4 r5 r6 r7 r8 r9 r10] );
52 temp_h11 = Temp ( [ini r1 r2 r3 r4 r5 r6 r7 r8 r9 r10] );
53
54 Time_c = Time(r10:last);
55 Temp_c = Temp(r10:last);
56 Kappa_c = Kappa(r10:last);
57 index = divide(Temp_c, 15);
58
59 time_c11 = Time_c ( index );
60 kappa_c11 = Kappa_c( index );
61 temp_c11 = Temp_c ( index );
62
63 [~,ini] = min( abs(Time - 331.8) );
64 [~,r1] = min( abs(Time - 343.8) );
65 [~,r2] = min( abs(Time - 354.1) );
66 [~,r3] = min( abs(Time - 365.3) );
67 [~,r4] = min( abs(Time - 378.6) );
68 [~,r5] = min( abs(Time - 390.1) );
69 [~,r6] = min( abs(Time - 399.2) );
70 [~,r7] = min( abs(Time - 410.1) );
71 [~,r8] = min( abs(Time - 422.6) );
72 [~,r9] = min( abs(Time - 433.9) );
73 [~,r10] = min( abs(Time - 443.9) );
74
75 time_h12 = Time ( [ini r1 r2 r3 r4 r5 r6 r7 r8 r9 r10] );
76 kappa_h12 = Kappa( [ini r1 r2 r3 r4 r5 r6 r7 r8 r9 r10] );
77 temp_h12 = Temp ( [ini r1 r2 r3 r4 r5 r6 r7 r8 r9 r10] );
78
79 Time_c = Time(r10:end);
80 Temp_c = Temp(r10:end);
81 Kappa_c = Kappa(r10:end);
82 index = divide(Temp_c, 15);
83
84 time_c12 = Time_c ( index );
85 kappa_c12 = Kappa_c( index );
86 temp_c12 = Temp_c ( index );
87
88 %% Curvature - Temperature Data
89
90 Time_h = {time_h11 time_h12};
91 Temp_h = {temp_h11 temp_h12};
92 Kappa_h = {kappa_h11 kappa_h12};
93
94 Time_c = {time_c11 time_c12};
95 Temp_c = {temp_c11 temp_c12};
96 Kappa_c = {kappa_c11 kappa_c12};
97
98 end

```

Appendix D

Cooling Stress Routine

```
1 % CTE Stresses cooling
2 %
3 % Matrix
4 % sigma_s_CTE(i,2) = Stress at the top and bottom of the substrate after
5 %                   the i-th temperature gradient
6 % sigma_d_CTE(i,j) = Stress at the midpoint of the j-th layer of the deposit
7 %                   after the i-th temperature gradient
8 % Vector
9 % E_d(j) = Young Modulus for the j-th layer
10 %
11 % Units: [Pa]
12
13 function [sigma_s_CTE, sigma_d_CTE, E_d] = CTE_Stress_c(N, w, a_d, E_d, ...
14             t_s, a_s, E_s, nu_s, Kappa, Temp_c)
15
16     % Parameters
17
18     E_s    = E_s/(1-nu_s);
19     t_d    = w./N;
20
21     dkappa = cell(1, length(N));
22     dtemp  = cell(1, length(N));
23
24     for i = 1:length(N)
25         dkappa{i} = diff(Kappa{i});
26         dtemp{i}  = diff(Temp_c{i});
27     end
28
29     % Elastic modulus assignation
30
31     E_d = young_moduli(N, E_d);
32
33     % Neutral axis position
34
35     delta = neutral_axis(N, t_d, E_d, t_s, E_s);
36
37     % Uniform strain component per temperature difference
38
39     uniform = strain_uniform(N, t_d, E_d, a_d, t_s, E_s, a_s);
```


Appendix E

Heating Stress Routine

```
1 % CTE Stresses heating
2 %
3 % Matrix
4 % sigma_s-CTE(i,2) = Stress at the top and bottom of the substrate after
5 % deposition of the i-th layer
6 % sigma_d-CTE(i,j) = Stress at the midpoint of the j-th layer of the deposit
7 % after deposition of the i-th layer
8 % Units: [Pa]
9 %
10 % Vector
11 % dkappa(j) = Change of curvature due to the j-th layer
12 % Units: [m^-1]
13
14
15 function [sigma_s-CTE, sigma_d-CTE, dkappa] = CTE-Stress_h(N, w, a_d, ...
16                                     E_d, t_s, a_s, E_s, nu_s, Temp_h)
17     % Parameters
18
19     E_s = E_s/(1-nu_s);
20
21     dtemp = cell(1, length(N));
22
23     for i = 1:length(N)
24         dtemp{i} = diff(Temp_h{i});
25     end
26
27     t_d = w./N;
28
29     % Neutral axis position
30
31     delta = neutral_axis(N, t_d, E_d, t_s, E_s);
32
33     % Uniform strain component per temperature difference
34
35     uniform = strain_uniform(N, t_d, E_d, a_d, t_s, E_s, a_s);
36
37     % Curvature change due to temperature difference
38
39     dkappa = curvature(N, t_d, E_d, a_d, t_s, E_s, a_s, dtemp, uniform, delta);
```


Appendix F

Evolving Stress Routine

```
1 % Intrinsic Stresses
2 % Matrix
3 % sigma_s(i,2) = Stress at the top and bottom of the substrate after
4 %               deposition of the i-th layer
5 % sigma_d(i,j) = Stress at the midpoint of the j-th layer of the deposit
6 %               after deposition of the i-th layer
7 % Units: [Pa]
8
9 function [sigma_s, sigma_d] = EvolvingStress(N, w, E_d, t_s, E_s, ...
10                                           nu_s, Kappa_h, dkappa_h)
11     % Parameters
12
13     E_s    = E_s/(1-nu_s);
14     t_d    = w./N;
15     dkappa = cell(1, length(N));
16     for i = 1:length(N)
17         dkappa{i} = diff(Kappa_h{i}) - dkappa_h{i};
18     end
19
20     % Neutral axis position
21
22     delta = neutral_axis(N, t_d, E_d, t_s, E_s);
23
24     % Composite beam stiffness per width
25
26     Sigma_b = stiff(N, t_d, E_d, t_s, E_s, delta);
27
28     % Tensile/Compressive force per width
29
30     F_b = force(N, t_d, t_s, dkappa, delta, Sigma_b);
31
32     % Stress distribution on the substrate
33
34     sigma_s = stress_sust(N, t_d, E_d, t_s, E_s, dkappa, delta, F_b);
35
36     % Stress distribution on the deposit
37
38     sigma_d = stress_depo(N, t_d, E_d, t_s, E_s, dkappa, delta, F_b);
39 end
```

Appendix G

Intrinsic Stress Routine

```
1 % Quenching Stress
2 % Vector
3 % sigma_q(i) = quenching stress at the layer i
4 % sigma_st(i) = Stoney approximation stress at the layer i
5 % Units: [Pa]
6
7 function [sigma_q, sigma_st] = Intrinsic(N, w, E_d, t_s, E_s, nu_s, ...
8                                             Kappa_h, dkappa_h)
9
10 % Parameters
11
12 E_s = E_s/(1-nu_s);
13 t_d = w./N;
14 dkappa = cell(1, length(N));
15
16 for i = 1:length(N)
17     dkappa{i} = diff(Kappa_h{i}) - dkappa_h{i};
18 end
19
20 % Neutral axis position
21
22 delta = neutral_axis(N, t_d, E_d, t_s, E_s);
23
24 % Composite beam stiffness per width
25
26 Sigma_b = stiff(N, t_d, E_d, t_s, E_s, delta);
27
28 % Tensile/Compressive force per width
29
30 F_b = force(N, t_d, t_s, dkappa, delta, Sigma_b);
31
32 % Quenching Stress
33
34 sigma_q = quench(N, t_d, E_d, t_s, E_s, F_b);
35
36 % Stoney approximation
37
38 sigma_st = stoney(N, t_d, t_s, E_s, dkappa);
39 end
```

Appendix H

Plotting Results Routine

```
1 % Plotting Results
2
3 function Plot_Result(N, w, t_s, sigma_s, sigma_d, sigma_s_h, sigma_d_h, ...
4     sigma_s_c, sigma_d_c, Sigma_q, Sigma_st, Process, filename)
5
6     [Time, Temp, Kappa, Time_h, Temp_h, Kappa_h, Time_c, Temp_c, Kappa_c] ...
7         = Read_Data2(filename);
8
9     y_s = [-t_s 0];
10    h_0 = 0;
11    t_d = w./N;
12
13    sigma_s = sigma_s + sigma_s_h;
14    sigma_d = sigma_d + sigma_d_h;
15
16    y_d = [];
17
18    time_h = [];
19    temp_h = [];
20    kappa_h = [];
21
22    time_c = [];
23    temp_c = [];
24    kappa_c = [];
25
26    sigma_q = [];
27    sigma_ev = [];
28
29    for i = 1:length(N)
30
31        h_n = h_0 + N(i)*t_d(i);
32        y_d = [y_d, h_0 + t_d(i)/2:t_d(i):h_n - t_d(i)/2];
33        h_0 = h_n;
34
35        time_h = [time_h; Time_h{i}];
36        temp_h = [temp_h; Temp_h{i}];
37        kappa_h = [kappa_h; Kappa_h{i}];
38
39        time_c = [time_c; Time_c{i}];
```



```

40     temp_c = [temp_c; Temp_c{i}];
41     kappa_c = [kappa_c; Kappa_c{i}];
42
43     sigma_q = [sigma_q; Sigma_q{i}];
44     sigma_ev = [sigma_ev; Sigma_st{i}];
45
46 end
47
48 % Curvature Plot
49
50 figure
51 plot(Time , Kappa, black , ...
52      time_h, kappa_h, *b , ...
53      time_c, kappa_c, *b )
54 title(Process, fontsize ,20, FontWeight , bold , Interpreter , latex )
55 xlabel( Time (s) , fontsize , 18, Interpreter , latex )
56 ylabel( Curvature (m-1) , fontsize , 18, Interpreter , latex )
57 legend1 = legend( Experimental , In the model );
58 set(legend1, Interpreter , latex , FontSize ,14)
59 grid on
60
61 % Temperature Plot
62
63 figure
64 plot(Time , Temp, black , ...
65      time_h, temp_h, *b , ...
66      time_c, temp_c, *b )
67 title(Process, fontsize ,20, FontWeight , bold , Interpreter , latex )
68 xlabel( Time (s) , fontsize , 18, Interpreter , latex )
69 ylabel( Temperature (°C) , fontsize , 18, Interpreter , latex )
70 legend1 = legend( Experimental , In the model );
71 set(legend1, Interpreter , latex , FontSize ,14)
72 grid on
73
74 % Coat_Final Stresses Plot
75
76 figure
77 hold on
78 h1 = plot( y_s*1e3, sigma_s(end,:)*1e-6, red );
79 plot( y_d*1e3, sigma_d(end,:)*1e-6, red );
80 h2 = plot( y_s*1e3, sigma_s_c(end,:)*1e-6, blue );
81 plot( y_d*1e3, sigma_d_c(end,:)*1e-6, blue );
82 h3 = plot( y_s*1e3, (sigma_s(end,:)+sigma_s_c(end,:))*1e-6, black );
83 plot( y_d*1e3, (sigma_d(end,:)+sigma_d_c(end,:))*1e-6, black );
84 title(Process, fontsize ,20, FontWeight , bold , Interpreter , latex )
85 xlabel( Distance from Interface (mm) , fontsize ,18, Interpreter , latex )
86 ylabel( Residual Stress (MPa) , fontsize ,18, Interpreter , latex )
87 leg1 = legend([h1,h2,h3], Coating Stress , Post-Dep. Stress , Final Stress );
88 set(leg1, Interpreter , latex , FontSize ,14)
89 grid on
90
91 % Stoney Formula Comparison
92
93 figure
94 plot(y_d*1e3, sigma_q*1e-6, black , ...
95      y_d*1e3, sigma_ev*1e-6, blue )
96 title(Process, fontsize ,20, FontWeight , bold , Interpreter , latex )
97 xlabel( Distance from Interface (mm) , fontsize ,18, Interpreter , latex )
98 ylabel( Intrinsic Stress (MPa) , fontsize ,18, Interpreter , latex )

```

```
99     legend1 = legend( Linear-elastic Model , Stoney Approx. );
100     set(legend1, Interpreter , latex , FontSize ,12)
101     grid on
102 end
```

Appendix I

Subroutines for Thermal Stress Distribution

I.1 Young modulus assignation

```
1 % Young Modulus assignation
2 % Vector
3 % E_d(i) = Elastic Modulus for the layer i
4 % Units: [Pa]
5
6 function E_d = young_moduli(N, E)
7
8     E_d = cell(1, length(N));
9
10    for i = 1:length(N)
11
12        E_d{i} = E(i)*ones(N(i),1);
13
14    end
15 end
```

I.2 Neutral axis position

```
1 % Neutral Axis Position
2 % Vector
3 % delta(i) = Neutral axis after deposition of the i-th layer
4 % Units: [m]
5
6 function delta = neutral_axis(N, t_d, E_d, t_s, E_s)
7
8     sum1 = 0;
9     sum2 = 0;
10    h_0 = 0;
```

```

11     h_n    = 0;
12     delta = cell(1:length(N));
13
14     for i=1:length(N)
15
16         h_n    = h_n(end) + t_d(i)*(1:N(i)) ;
17         h_ant  = [h_0; h_n(1:end-1)];
18         h_0    = h_n(end);
19
20         sum1   = sum1(end) + t_d(i)*cumsum( E_d{i}.*(2*h_ant + t_d(i)) );
21         sum2   = sum2(end) + t_d(i)*cumsum( E_d{i} );
22
23         delta{i} = ( -E_s*t_s^2 + sum1 ) ./ ( 2*(E_s*t_s + sum2) );
24
25     end
26 end

```

I.3 Uniform strain component

```

1  % Uniform misfit strain per temperature difference
2  % Vector
3  % uniform(i) = Strain due to the temperature difference i
4  % Units: [C^-1]
5
6  function uniform = strain_uniform(N, t_d, E_d, a_d, t_s, E_s, a_s)
7
8      sum1    = 0;
9      sum2    = 0;
10     uniform = cell(1,length(N));
11
12     for i=1:length(N)
13         sum1 = sum1(end) + t_d(i)*a_d(i)*cumsum( E_d{i} );
14         sum2 = sum2(end) + t_d(i)*cumsum( E_d{i} );
15
16         uniform{i} = ( E_s*t_s*a_s + sum1 ) ./ ( E_s*t_s + sum2 );
17
18     end
19 end

```

I.4 Curvature

```

1  % Curvature
2  % Vector
3  % dkappa(i) = Curvature change after deposition/temperature gradient i
4  % Units: [m^-1]
5
6  function dkappa = curvature(N, t_d, E_d, a_d, t_s, E_s, a_s, dtemp, ...
7                               uniform, delta)
8
9      sum1    = 0;

```

```

10     sum2     = 0;
11     h_0     = 0;
12     h_n     = 0;
13     dkappa  = cell(1, length(N));
14
15     for i = 1:length(N)
16
17         h_n   = h_n(end) + t_d(i)*(1:N(i));
18         h_ant = [h_0; h_n(1:end-1)];
19         h_0   = h_n(end);
20
21         sum1 = sum1(end) + cumsum( E_d{i}.*(2*h_ant + t_d(i)) );
22         sum2 = sum2(end) + cumsum( E_d{i}.*(3*h_ant.^2 + 3*h_ant*t_d(i) + ...
23                                 t_d(i)^2) );
24
25         num = 3*dtemp{i}.*( t_s^2*( uniform{i} - a_s )*E_s - ...
26                             t_d(i)*( uniform{i} - a_d(i) ).*sum1 );
27         den = 2*t_s^3*E_s + 3*t_s^2*delta{i}*E_s + ...
28             2*t_d(i)*sum2 - 3*t_d(i)*delta{i}.*sum1;
29
30         dkappa{i} = - num ./ den;
31
32     end
33 end

```

I.5 Stress distribution in substrate

```

1  % Stress distribution in the substrate due to temperature difference
2  % Matrix
3  % sigma_sust_CTE(i,2) = Stress at the top and bottom of the substrate due
4  %                     to the temperature difference i
5  % Units: [Pa]
6
7  function sigma_sust_CTE = stress_sust_CTE(N, E_s, a_s, t_s, uniform, ...
8                                         delta, dkappa, dtemp)
9
10     y     = [-t_s 0];
11     col   = length(y);
12     sigma = zeros(1, col);
13
14     sigma_s_CTE = cell(1, length(N));
15
16     for i = 1:length(N)
17
18         row   = length(dtemp{i});
19         dsigma = zeros(row, col);
20
21         if sum(dtemp{1}) < 0
22
23             for j = 1:col
24
25                 depsilon = uniform{i}(end)*dtemp{i} - ...
26                         (y(j) - delta{i}(end)).*dkappa{i};
27                 dsigma(:, j) = E_s*(depsilon - a_s*dtemp{i});

```

```

28
29         end
30     else
31
32         for j = 1:col
33
34             depsilon = uniform{i}.*dtemp{i} - ...
35                 (y(j) - delta{i}).*dkappa{i};
36             dsigma(:,j) = E_s*(depsilon - a_s*dtemp{i});
37
38         end
39     end
40
41     sigma = ones(row, 1)*sigma(end,:) + cumsum(dsigma);
42
43     sigma_s_CTE{i} = sigma;
44
45 end
46
47 sigma_sust_CTE = [];
48
49 for i = 1:length(N)
50
51     sigma_sust_CTE = [ sigma_sust_CTE; sigma_s_CTE{i} ];
52
53 end
54 end

```

I.6 Stress distribution in deposit

```

1 % Stress distribution in the deposit due to temperature difference
2 % Matrix
3 % sigma_d.CTE(i,j) = Stress at midpoint of layer j due to the temperature
4 %                   difference i
5 % Units: [Pa]
6
7 function sigma_d_CTE = stress_depo_CTE(N, E_D, a_D, t_d, Uniform, Delta, ...
8                                     Dkappa, Dtemp)
9
10     h_0 = 0;
11
12     y = [];
13     dtemp = [];
14     dkappa = [];
15     E_d = [];
16     a_d = [];
17     uniform = [];
18     uniform_c = [];
19     delta = [];
20     delta_c = [];
21
22     for i = 1:length(N)
23
24         h_n = h_0 + N(i)*t_d(i);

```

```

25     y    = [y, h_0 + t_d(i)/2:t_d(i):h_n - t_d(i)/2];
26     h_0 = h_n;
27     n    = length(Dtemp{i});
28
29     dtemp    = [dtemp; Dtemp{i}];
30     dkappa   = [dkappa; Dkappa{i}];
31     E_d      = [E_d E_D{i}];
32     a_d      = [a_d a_D(i)*ones(1,N(i))];
33     uniform   = [uniform; Uniform{i}];
34     uniform_c = [uniform_c; Uniform{i}(end)*ones(n,1)];
35     delta    = [delta; Delta{i}];
36     delta_c  = [delta_c; Delta{i}(end)*ones(n,1)];
37
38     end
39
40     row    = length(dtemp);
41     col    = length(y);
42     dsigma = zeros(row,col);
43
44     if sum(Dtemp{1}) < 0
45
46         for j = 1:col
47
48             depsilon    = uniform_c.*dtemp - (y(j) - delta_c).*dkappa;
49             dsigma(:,j) = E_d(j)*(depsilon - a_d(j)*dtemp);
50
51             end
52         else
53
54             for j = 1:col
55
56                 depsilon    = uniform.*dtemp - (y(j) - delta).*dkappa;
57                 dsigma(:,j) = E_d(j)*(depsilon - a_d(j)*dtemp);
58
59             end
60
61             dsigma = tril( dsigma );
62
63         end
64
65     sigma_d_CTE = cumsum(dsigma);
66
67     end

```

Appendix J

Subroutines for Intrinsic Stress Distribution

J.1 Composite beam stiffness

```
1 % Composite Beam Stiffness per width
2 % Vector
3 % Sigma_b(i) = Beam stiffness per width after deposition of layer i
4 % Units: [Pa*m^3]
5
6 function Sigma_b = stiff(N, t_d, E_d, t_s, E_s, delta)
7
8     sum1 = 0;
9     sum2 = 0;
10    sum3 = 0;
11    h_0 = 0;
12    h_n = 0;
13    Sigma_b = cell(1, length(N));
14
15    for i = 1:length(N)
16
17        h_n = h_n(end) + t_d(i)*(1:N(i));
18        h_ant = [h_0; h_n(1:end-1)];
19        h_0 = h_n(end);
20
21        sum1 = sum1(end) + cumsum( E_d{i}.*(h_n.^2 + h_n.*h_ant + h_ant.^2) );
22        sum2 = sum2(end) + cumsum( E_d{i}.*(h_n + h_ant) );
23        sum3 = sum3(end) + cumsum( E_d{i} );
24
25        Sigma_b{i} = E_s*t_s*( t_s^2/3 + t_s*delta{i} + delta{i}.^2 ) + ...
26                        t_d(i)*( sum1/3 - sum2.*delta{i} + sum3.*delta{i}.^2 );
27
28    end
29 end
```


J.2 Tensile/Compressive force

```

1 % Tensile/Compressive force per width
2 % Vector
3 % F(i) = Tensile/Compressive force per width developed during application
4 %       of layer i
5 % Units: [N/m]
6
7 function F_b = force(N, t_d, t_s, dkappa, delta, Sigma_b)
8
9     h_0     = 0;
10    h_n     = 0;
11    delta_0 = -t_s/2;
12    F_b     = cell(1, length(N));
13
14    for i = 1:length(N)
15
16        h_n = h_n(end) + t_d(i)*(1:N(i));
17        h_ant = [h_0; h_n(1:end-1)];
18        h_0 = h_n(end);
19
20        delta_ant = [delta_0; delta{i}(1:end-1)];
21        delta_0 = delta{i}(end);
22
23        F_b{i} = ( Sigma_b{i}.*dkappa{i} ) ./ ...
24                ( h_ant - delta_ant + t_d(i)/2 );
25
26    end
27 end

```

J.3 Stress distribution in substrate

```

1 % Stress distribution on the substrate
2 % Matrix
3 % sigma_t(i,2) = Stress at the top and bottom of the substrate after
4 %              deposition of the i-th layer
5 % Units: [Pa]
6
7 function sigma_sust = stress_sust(N, t_d, E_d, t_s, E_s, dkappa, delta, F_b)
8
9     y     = [-t_s, 0];
10    col   = length(y);
11    equiv = t_s;
12    t_s_0 = t_s;
13    sigma = zeros(1, col);
14
15    sigma_s = cell(1, length(N));
16
17    for i = 1:length(N)
18
19        row = length(dkappa{i});
20        dsigma = zeros(row, col);

```

```

21
22     equiv    = equiv(end) + t_d(i)*cumsum( E_d{i} )/E_s;
23     t_equiv  = [ t_s_0; equiv(1:end-1) ];
24     t_s_0    = equiv(end);
25
26     for j = 1:col
27
28         dsigma(:,j) = - ( F_b{i} ./ t_equiv + E_s*dkappa{i}.* ...
29             ( y(j) - delta{i} ) );
30
31     end
32
33     sigma = ones(row, 1)*sigma(end,:) + cumsum(dsigma);
34
35     sigma_s{i} = sigma;
36
37 end
38
39 sigma_sust = [];
40
41 for i = 1:length(N)
42
43     sigma_sust = [ sigma_sust; sigma_s{i} ];
44
45 end
46 end

```

J.4 Stress distribution in deposit

```

1  % Stress distribution on the deposit
2  % Matrix
3  % sigma_d(i,j) = Stress at the midpoint of layer j after applying
4  %                layer i
5  % Units: [Pa]
6
7  function sigma_d = stress_depo(N, t_D, E_D, t_s, E_s, Dkappa, Delta, F_B)
8
9     h_0 = 0;
10
11     y      = [];
12     dkappa = [];
13     t_d    = [];
14     E_d    = [];
15     F_b    = [];
16     delta  = [];
17
18     for i = 1:length(N)
19
20         h_n = h_0 + N(i)*t_D(i);
21         y   = [y, h_0 + t_D(i)/2:t_D(i):h_n - t_D(i)/2];
22         h_0 = h_n;
23
24         dkappa = [dkappa; Dkappa{i}];
25         t_d    = [t_d t_D(i)*ones(1,N(i))];

```

```

26     E_d      = [E_d E_D{i} ];
27     F_b      = [F_b; F_B{i}];
28     delta    = [delta; Delta{i}];
29
30     end
31
32     row      = length(dkappa);
33     col      = length(y);
34     dsigma   = zeros(row,col);
35     bug      = zeros(row,col);
36     equiv    = E_s*t_s + cumsum( E_d(1:end-1).*t_d(1:end-1) );
37
38     for j = 1:col
39
40         dsigma(j,j) = - E_d(j)*dkappa(j)*(y(j) - delta(j)) + F_b(j)/t_d(j) ;
41
42         dsigma(j+1:end,j) = - ( F_b(j+1:end) ./ (equiv(j:end)/E_d(j)) + ...
43             E_d(j)*dkappa(j+1:end).*( y(j) - delta(j+1:end) ) );
44
45     end
46
47     sigma_d = cumsum(dsigma);
48
49 end

```

Appendix K

Subroutines for Quenching Stress Distribution

K.1 Quenching stress on deposit

```
1 % Quenching Stress acting on each layer
2 % Vector
3 % sigma_q(i) = Quenching stress at the layer i
4 % Units: [Pa]
5
6 function sigma_q = quench(N, t_d, E_d, t_s, E_s, F_b)
7
8     sum1 = 0;
9     ini = 0;
10
11     sigma_q = cell(1, length(N));
12
13     for i = 1:length(N)
14
15         sum1 = sum1 + cumsum( [ini; t_d(i)*E_d{i}(1:end-1)] );
16         Et_equiv = E_s*t_s + sum1;
17         ini = t_d(i)*E_d{i}(end);
18
19         sigma_q{i} = E_d{i}.*F_b{i}.*( Et_equiv.^(-1) + (E_d{i}*t_d(i)).^(-1) );
20
21         sum1 = sum1(end);
22
23     end
24 end
```

K.2 Stoney formula approximation

```
1 % Stoney formula approximation for quenching stress
2 % Vector
3 % sigma_q(i) = Stoney approximation stress at the layer i
4 % Units: [Pa]
5
6 function sigma_ev = stoney(N, t_d, t_s, E_s, dkappa)
7
8     sigma_ev = cell(1, length(N));
9
10    for i = 1:length(N)
11
12        sigma_ev{i} = E_s*t_s^2/6 * dkappa{i}/t_d(i);
13
14    end
15 end
```

Bibliography

- [1] David R. Clarke, Matthias Oechsner, and Nitin P. Padture. Thermal-barrier coatings for more efficient gas-turbine engines. *MRS Bulletin*, 37:891–898, 10 2012.
- [2] J.R. Davis and A.S.M.I.T.S.S.T. Committee. *Handbook of Thermal Spray Technology*. ASM International, 2004.
- [3] L. Pawlowski. *The Science and Engineering of Thermal Spray Coatings*. Wiley, 2008.
- [4] W.B. Choi, L. Li, V. Luzin, R. Neiser, T. Gnäupel-Herold, H.J. Prask, S. Sampath, and A. Gouldstone. Integrated characterization of cold sprayed aluminum coatings. *Acta Materialia*, 55(3):857 – 866, 2007.
- [5] O. Kesler, M. Finot, S. Suresh, and S. Sampath. Determination of processing-induced stresses and properties of layered and graded coatings: Experimental method and results for plasma-sprayed ni–al₂o₃. *Acta Materialia*, 45(8):3123 – 3134, 1997.
- [6] S Kuroda and TW Clyne. The quenching stress in thermally sprayed coatings. *Thin solid films*, 200(1):49–66, 1991.
- [7] C. Lyphout, P. Nylén, A. Manescu, and T. Pirling. Residual stresses distribution through thick hvof sprayed inconel 718 coatings. *Journal of Thermal Spray Technology*, 17(5-6):915–923, 2008.
- [8] J Matejcek and S Sampath. Intrinsic residual stresses in single splats produced by thermal spray processes. *Acta Materialia*, 49(11):1993 – 1999, 2001.
- [9] Alfredo Valarezo and Sanjay Sampath. An integrated assessment of process-microstructure-property relationships for thermal-sprayed nicr coatings. *Journal of Thermal Spray Technology*, 20(6):1244–1258, 2011.
- [10] J. Matejcek, S. Sampath, D. Gilmore, and R. Neiser. In situ measurement of residual stresses and elastic moduli in thermal sprayed coatings: Part 2: processing effects on properties of mo coatings. *Acta Materialia*, 51(3):873 – 885, 2003.

- [11] Seiji Kuroda, Yasuhiko Tashiro, Hisami Yumoto, Susumu Taira, Hirotaka Fukanuma, and Shogo Tobe. Peening action and residual stresses in high-velocity oxygen fuel thermal spraying of 316l stainless steel. *Journal of Thermal Spray Technology*, 10(2):367–374, 2001.
- [12] Y.C. Tsui and T.W. Clyne. An analytical model for predicting residual stresses in progressively deposited coatings part 1: Planar geometry. *Thin Solid Films*, 306(1):23 – 33, 1997.
- [13] C.H. Hsueh. Thermal stresses in elastic multilayer systems. *Thin Solid Films*, 418(2):182 – 188, 2002.
- [14] Giovanni Bolelli, Valeria Cannillo, Luca Lusvarghi, Roberto Rosa, Alfredo Valarezo, Wanhuk B. Choi, Ravi Dey, Christopher Weyant, and Sanjay Sampath. Functionally graded wc-co/nial {HVOF} coatings for damage tolerance, wear and corrosion protection. *Surface and Coatings Technology*, 206(8–9):2585 – 2601, 2012.